Titre: Title:	Bioconvection and thermo-bioconvection of gravitactic micro-organisms in enclosures
Auteur: Author:	Mehrdad Taheri
Date:	2007
Type:	Mémoire ou thèse / Dissertation or Thesis
Référence: Citation:	Taheri, M. (2007). Bioconvection and thermo-bioconvection of gravitactic micro-organisms in enclosures [Mémoire de maîtrise, École Polytechnique de Montréal]. PolyPublie. https://publications.polymtl.ca/7950/

UNIVERSITÉ DE MONTRÉAL

BIOCONVECTION AND THERMO-BIOCONVECTION OF GRAVITACTIC MICRO-ORGANISMS IN ENCLOSURES

MEHRDAD TAHERI
DÉPARTEMENT DE GÉNIE MÉCANIQUE
ÉCOLE POLYTECHNIQUE DE MONTRÉAL

MÉMOIRE PRÉSENTÉ EN VUE DE L'OBTENTION
DU DIPLÔME DE MAÎTRISE ÈS SCIENCES APPLIQUÉES
(GÉNIE MÉCANIQUE)
AVRIL 2007

Your file Votre référence
ISBN: 978-0-494-29258-7
Our file Notre référence
ISBN: 978-0-494-29258-7

UNIVERSITÉ DE MONTRÉAL

ÉCOLE POLYTECHNIQUE DE MONTRÉAL

Ce mémoire intitulé:

BIOCONVECTION AND THERMO-BIOCONVECTION OF GRAVITACTIC MICRO-ORGANISMS IN ENCLOSURES

présenté par: TAHERI Mehrdad

en vue de l'obtention du diplôme de: Maîtrise ès sciences appliquées

a été dûment accepté par le jury d'examen constitué de:

M. ROBILLARD Luc, D.Sc., président

M. BILGEN Ertugrul, Ph.D., membre et directeur de recherche

M. VO Huu Duc, Ph.D., membre

Acknowledgments

I would like to express my gratitude to all of those who gave me the possibility to complete this thesis. First, I wish to express my sincere thanks to my supervisor, Professor Ertugrul Bilgen, who provided me the opportunity to pursue my Master's degree. His thoughtful instructions and wise advice at each step of this research have always shed some light on my way to pursue this work. Next, I would like to thank committee members: Professor Luc Robillard and Professor Huu Duc Vo for their critical comments to improve this thesis. Also, I want to thank my former colleagues and friends at Mechanical Engineering Department of Ecole Polytechnique de Montreal, especially Herve-Frank Nouanegue, for their help, support, and valuable hints.

In addition, I would like to express my sincere appreciation and thanks to my parents Farideh Nalbandi, and Mohammad Taheri, and my brothers Morteza and Mahyar Taheri for being enduring, encouraging and caring to my aspirations. Finally, I would like to thank my friends: Sara Fadaee, Forough Ensandoust, Bahador Bakhtiari, and my other friends who endured this process with me, always offering support and love. To them, I dedicate this thesis.

Résumé

Cette thèse se propose d'étudier la bioconvection gravitactique dans des cavités rectangulaires et cylindriques. Pour une cavité rectangulaire les effets du nombre de Peclet de bioconvection et du rapport de forme sont étudiés sur le début de la bioconvection. Les cavités rectangulaires sont avec des parois rigides et imperméables. En outre, la condition d'adhérence aux parois verticales ne s'applique pas. Le nombre de Peclet varie de 0.1 à 10 et le rapport de forme de 1 à 5. Dans le cas d'un cylindre vertical, l'effet du chauffage ou du refroidissement par le bas à la température ou au flux constant sur le développement de bioconvection gravitactique a été étudiée. Les parois des cylindres verticaux sont avec des parois rigides, imperméables et adiabatiques, mais la condition d'adhérence ne s'applique pas. Par contre, les parois horizontales sont rigides, imperméables et la condition d'adhérence s'applique. Le nombre de Peclet varie de 1 à 10, et le rapport de forme de 0.2 à 1.

Dans le cas de bioconvection, les équations modélisant le phénomène sont la continuité, les équations de Navier-Stokes avec l'approximation de Boussinesq, l'équation de diffusion pour les micro-organismes mobiles et dans le cas thermo-bioconvection, l'équation d'énergie est aussi incluse. La méthode des volumes de contrôle est employée pour résoudre numériquement le système des équations avec les conditions aux frontières appropriées.

Dans le cas de bioconvection dans des cavités rectangulaires, nos résultats montrent l'influence du nombre de Peclet de bioconvection et du rapport de forme sur le diagramme de bifurcation et la structure d'écoulement. Nous avons trouvé que la bifurcation demeure sous-critique dans tous les cas quand le nombre de Peclet de bioconvection varie de 0.1 à 10 dans des cavités rectangulaires ayant un rapport de forme de 1 à 5. Le nombre de Rayleigh critique diminue avec l'augmentation du nombre de Peclet de bioconvection et aussi avec l'augmentation du rapport de forme.

Dans le cas de thermo-bioconvection dans des cavités cylindriques, les résultats montrent l'influence de l'effet du chauffage et du refroidissement par le bas sur le diagramme de bifurcation et le contour de la bioconvection gravitactique. Nous avons constaté que les bifurcations sous-critiques de la bioconvection deviennent supercritiques quand le nombre de Rayleigh thermique est différent de zéro. Pour $Ra_T < 0$, c.-à-d. pour le refroidissement par le bas, nous avons des forces de flottabilité opposantes, la convection décroit et le nombre de Rayleigh critique du thermo-bioconvection augmente par rapport à celui de la bioconvection. Pour $Ra_T > 0$, c.-à-d. pour le cas du chauffage par le bas, les forces de flottabilité sont coopérantes et la convection augmente et le nombre de Rayleigh critique de thermo-bioconvection diminue par rapport à celui de la bioconvection.

Abstract

This thesis investigates the gravitactic bioconvection in rectangular and cylindrical enclosures. In case of rectangular cavities, the effects of bioconvection Peclet number and aspect ratio are investigated on the onset of bioconvection. The Peclet number varied from 0.1 to 10 and the aspect ratio from 1 to 5. In the vertical cylinder case, the effect of heating or cooling from below at constant temperature and constant heat flux on the development of gravitactic bioconvection is studied in vertical cylinders with stress free sidewalls, and top and bottom rigid walls. The Peclet number changed from 1 to 10 and aspect ratio from 0.2 to 1.

The governing equations for bioconvection are the continuity, the Navier-Stokes equations with the Boussinesq approximation, the diffusion equation for the motile micro-organisms and in case of thermo-bioconvection, they include also the energy equation. The control volume method is used to solve numerically the complete set of governing equations.

In case of bioconvection in rectangular cavities, the present results exhibit the influence of bioconvection Peclet number and aspect ratio on the bifurcation diagram and the flow structure. We have found that the bifurcation remains subcritical in all cases when the bioconvection *Pe* number is varied from 0.1 to 10 in rectangular enclosures having an

aspect ratio from 1 to 5. The critical Rayleigh number is decreased with increasing bioconvection Peclet number and with increasing aspect ratio.

In case of thermo-bioconvection in cylindrical cavities, the results show the influence of thermal effect on the bifurcation diagram and the pattern of gravitactic bioconvection. We found that subcritical bifurcations of bioconvection became supercritical bifurcations when the thermal Rayleigh number Ra_T is different than zero. For $Ra_T < 0$, i.e. for cooling from below, we have opposing buoyancy forces, the convection is decreased and the critical thermo-bioconvection Rayleigh number is increased with respect to that of bioconvection. For $Ra_T > 0$, i.e. for heating from below, we have cooperating buoyancy forces, the convection is increased and the critical thermo-bioconvection Rayleigh number is decreased with respect to that of bioconvection.

Condensé

Le but de ce mémoire de maîtrise est d'étudier la bioconvection gravitactique des micro-organismes dans les cavités. Nous étudions la bioconvection dans des cavités rectangulaires avec les parois rigides et imperméables. Pour examiner la thermo-bioconvection, nous allons considérer des cylindres verticaux et étudier l'effet du chauffage et du refroidissement par le bas à la température ou au flux constant sur la bioconvection.

La bioconvection est la formation spontanée d'un mouvement dans les suspensions des micro-organismes, qui sont un peu plus denses que l'eau et se déplacent aléatoirement, mais avec un mouvement global de bas vers le haut, dans le sens contraire de la pesanteur. Le mouvement ascendant des micro-organismes est généralement une réponse à un champ de force externe tel que la pesanteur (le gravitaxe ou le géotaxe), une source lumineuse (phototaxe), un stimulus biochimique tel que le gradient de la concentration en oxygène (chemotaxes) et des couples de force dus à la pesanteur et au cisaillement (gyrotaxes). En raison du mouvement ascendant, la couche supérieure de la suspension devient plus dense que la couche inférieure, résultant en une distribution instable de densité. Ceci peut mener à une convection instable et à la formation de convection semblable à la convection de Rayleigh-Bénard.

Des modèles théoriques du bioconvection pour différents types de micro-organismes motiles ont été développés dans diverses publications récentes et, une analyse du travail fondamental dans ce secteur a été publiée. Des modèles rationnels de continuum pour une suspension des micro-organismes purement gravitactiques ont été formulés et analysés par Childress et al. Cette formulation inclut les équations de Navier-Stokes avec l'approximation de Boussinesq pour les fluides incompressibles et l'équation de la conservation de micro-organismes. Les diverses études basées sur les équations formulées par Childress et al. ont été présentées par Fujita & Watanabe, et Harashima et al. Ils ont constaté que le système de la bioconvection peut avoir un comportement chaotique par l'intermédiaire d'une séquence des bifurcations lorsque le nombre de Rayleigh augmente et ainsi le système évolue dans la direction de l'advection descendante plus forte des micro-organismes et celui de la minimisation de l'énergie potentielle du système.

La revue de littérature montre qu'il n'y a, jusqu'ici, aucune simulation numérique de la bioconvection dans des cavités rectangulaires et des écoulements de thermo-bioconvection au-dessus des nombres Rayleigh critiques, toutes les études ont seulement considéré les solutions analytiques du problème de stabilité. Par conséquent, nous avons dans ce mémoire, deux études distinctes ; la première est sur la bioconvection des micro-organismes gravitactiques dans des cavités rectangulaires et la seconde sur la thermo-bioconvection des micro-organismes gravitactiques dans des cylindres verticaux.

Cette thèse est présentée en 5 chapitres. Le chapitre 1 présente la bioconvection. Elle contient la définition du problème et passe en revue brièvement les travaux précédents effectués sur le sujet. Dans le chapitre 2, le modèle mathématique utilisé pour résoudre le problème est décrit. Ce chapitre inclut 3 sections; dans la première section le modèle mathématique et les équations de la bioconvection dans une cavité rectangulaire sont exposées. Dans la deuxième partie, les équations régissantes la thermo-bioconvection sont présentées en coordonnées cylindriques. Dans la dernière partie, la méthode numérique employée pour résoudre le problème est exposée. Le chapitre 3 présente les résultats et les discussions pour le problème de la bioconvection dans des cavités rectangulaires. Le chapitre 4 discute les résultats obtenus pour la thermo-bioconvection dans des cylindres verticaux. Le chapitre 5 donne les conclusions générales de cette étude.

Dans la première partie de ce mémoire, nous nous concentrons sur la bioconvection gravitactique développée dans une solution des micro-organismes gravitactiques, comme la paramécie et le tetrahymena, dans les cavités carrées à rectangulaire avec différents rapport de formes. Les paramètres influant sont Sc = 1, Pe = 0.1-10 et A = 1-5. Nous obtenons les solutions numériques aux équations régissantes : les équations de la continuité, de Navier-Stokes complètes et de la concentration des cellules avec conditions critiques au début de la convection. Notre but a été d'étudier les effets du rapport de forme et du nombre de Peclet sur le commencement et le développement de la bioconvection.

Dans la deuxième étude, nous effectuons une recherche numérique sur le développement de la thermo-bioconvection dans des cylindres verticaux avec les parois latérales adiabatiques et imperméables. Nous nous concentrons sur l'effet du chauffage ou du refroidissement le bas dans les cas (i) d'isotherme et (ii) du isoflux, et nous étudions l'effet thermique sur les caractéristiques de bifurcation des micro-organismes gravitactiques.

En cas de la bioconvection dans des cavités rectangulaires, le système se compose d'une solution de micro-organismes gravitactiques inclus dans des cavités rectangulaires bidimensionnelles de largeur L et hauteur H référant aux coordonnées cartésiennes (x', y') avec l'axe y' se dirigeant verticalement vers le haut. Initialement, nous avons une distribution uniforme de concentration $\bar{n}$ et chaque cellule a un volume ϑ et une densité ρ_c. Nous supposons que la solution est incompressible et l'approximation de Boussinesq s'applique. L'approximation de Boussinesq suppose que toutes les propriétés physiques sont constantes, excepté la densité dans les termes des flottabilités, qui peut être exprimée comme fonction linéaire de concentration des cellules. L'équation de quantité de mouvement sous l'approximation de Boussinesq mène à l'équation de vorticité. Nous imposons des conditions limites rigides avec la condition d'adhérence aux parois supérieure et inférieure, mais pas aux parois latérales. En outre, il n'y a aucun flux de cellule à travers les parois rigides. Les paramètres régissant sont le nombre de Schmidt $Sc = \nu / D_c$, le nombre de Peclet de la bioconvection $Pe = V_c H / D_c$ et le nombre de Rayleigh de bioconvection $Ra = g\vartheta\bar{n}\Delta\rho H^3 / \rho\nu D_c$.

Dans le cas de thermo-bioconvection dans des cylindres verticaux, le système se compose d'une solution des micro-organismes gravitactiques dans des cavités cylindriques du rayon R et de la hauteur H en référence aux coordonnées cylindriques *(r, z)* avec l'axe de z se dirigeant verticalement vers le haut. Les parois des cylindres sont rigides et imperméables. De plus, les parois verticales de la cavité sont adiabatiques et la condition d'adhérence ne s'applique pas. Il n'y a aucun flux des cellules à travers les murs. Nous supposons le fluide incompressible et l'écoulement axisymétrique. La distribution de la concentration est uniforme et chaque cellule a un volume ϑ et une densité ρ_c. Les équations bidimensionnelles de Navier-Stokes avec l'approximation de Boussinesq, l'équation de conservation de cellules et l'équation de l'énergie sont résolues. Les paramètres régissant du problème sont, le nombre de Schmidt $Sc = \nu / D_c$, le nombre de Peclet de la bioconvection $Pe = HV_c / D_c$ le nombre de Rayleigh de bioconvection, $Ra = g\vartheta \bar{n} \Delta\rho H^3 / \rho \nu D_c$ et les nombres de Rayleigh thermique $Ra_T = g\beta\Delta T H^3 / \nu\alpha$ et $Ra_T = g\beta q H^4 / \nu\alpha k$, et le nombre de Lewis $Le = \alpha / D_c$.

Pour résoudre le système d'équations résultant, nous avons utilisé la méthode de volumes de contrôle. Les équations régissantes sont discrétisées avec une grille uniforme décalée avec la fonction de courant stockée sur un ensemble de nœuds et la vorticité et la concentration stockées sur un autre ensemble de nœuds. Les équations discrétisées sont dérivées en utilisant les différences centrales pour les dérivées spatiales et des différences arrières pour des dérivées temporelles. Un algorithme ligne par ligne de matrice

tridiagonale avec la relaxation est employé conjointement avec une méthode itérative pour résoudre les équations discrétisées non-linéaires.

Le programme numérique a été validé par rapport à la convection thermique, à la bioconvection et à la diffusion double disponible dans la littérature. Un maillage uniforme dans la direction de x et de y est employé pour tous les calculs. La convergence en fonction du maillage est étudiée pour différents cas, et la taille appropriée du maillage pour chaque cas est utilisée pour tous les calculs de la présente étude.

Dans l'étude de bioconvection, des calculs ont été effectués en utilisant les gammes suivantes des paramètres pour l'étude de bioconvection : le rapport de forme (de A = 1, 2 et 5), le nombre de Peclet de bioconvection, (Pe = 0.1, 1 et 10), le nombre de Schmidt Sc = 1 et le nombre de Rayleigh. Les nombres de Pe et de Sc correspondent aux cas de bioconvection avec micro-organismes typiques : le coefficient de diffusion D_c = $5\text{x}10^{-3}$ - $0.5\text{x}10^{-2}$ cm^2/s, la vitesse de cellules V_c = $7.5\text{x}10^{-3}$ - $1\text{x}10^{-2}$ cm/s , densité de cellules ρ_c = (1.035 -1.10) ρ_w, le volume de cellules υ = $1\text{x}10^{-12}$ - $5\text{x}10^{-10}$ cm^3, la concentration de cellules = $8.44\text{x}10^5$ - $1\text{x}10^9$ $cell/cm^3$. Par exemple, pour le caudatum de paramécie, D_c = $5\text{x}10^{-3}$ - $4.5\text{x}10^{-2}$ cm^2/s, V_c = $3.2\text{x}10^{-2}$ - $7.7\text{x}10^{-2}$ cm/s, H = 0.1 centimètre ; nous obtenons Sc = 0.22 - 2 et Pe = 0.07 - 1.54.

Les résultats ont montré l'influence du nombre de Peclet de bioconvection et du rapport de forme sur le diagramme de bifurcation et la structure de l'écoulement. Nous avons

constaté que la bifurcation demeure sous-critique dans tous les cas quand le nombre de *Pe* de bioconvection varie entre 0.1 et 10 dans les cavités rectangulaires ayant un rapport de forme de 1 à 5. Pour le cas de thermo-bioconvection, les calculs ont été exécutés avec le rapport de forme de A = 1, 0.5, 0.2 et des valeurs variables de Ra et Ra_T pour des paramètres sans dimensions suivantes : Sc = 1, Le = 1, Pe = 1 et 10, qui correspondent aux cas typiques de bioconvection avec caractéristiques connues de micro-organismes. D'abord, nous avons obtenu des courbes de bifurcation par simulation numérique, les nombres critiques de Rayleigh thermiques, Ra_{Tc} sans bioconvection, c.-à-d. avec Ra = 0. Puis, nous avons obtenu des courbes de bifurcation par simulation numérique, les nombres sous-critiques de Rayleigh de bioconvection, Ra_c sans effet thermique, c.-à-d. avec Ra_T = 0. En conclusion, en employant les nombres critiques de Rayleigh thermiques et les nombres sous-critiques de Rayleigh de bioconvection, nous avons étudié par la simulation numérique pour obtenir des courbes de bifurcation pour déterminer les nombres de Rayleigh critiques pour les cas $Ra_T = 1 \times Ra_{Tc}$, et $2 \times Ra_{Tc}$ (c.-à-d. chauffage par le bas) et au $Ra_T = -1 \times Ra_{Tc}$, $-2 \times Ra_{Tc}$ (c.-à-d. refroidissement par le bas) avec les conditions de T = constante et q = constante.

Les résultats montrent l'influence de l'effet thermique sur le diagramme de bifurcation et le modèle de la bioconvection gravitactique. Nous avons constaté que les bifurcations sous-critiques de la bioconvection deviennent supercritiques quand le nombre de Rayleigh thermique Ra_T est différent de zéro. Pour $Ra_T < 0$, c.-à-d. pour le refroidissement par le bas, nous avons les forces de flottabilité oppossantes. La

convection diminue, les courbes de concentration sont modifiées pour refléter le changement du champ d'écoulement, et le nombre de Rayleigh critique de thermo-bioconvection augmente par rapport à celui de la bioconvection. Pour $Ra_T > 0$, c.-à-d. pour le cas de chauffage par le bas, nous avons les forces de flottabilité coopérantes, la convection augmente, les courbes de concentration sont modifiées, et le nombre de Rayleigh critique de thermo-bioconvection diminue par rapport à celui de la bioconvection. Nous avons donc trouvé que tant le chauffage par le bas que refroidissement par le bas avec la température ou le flux constante nous avons un effet déstabilisant sur la bioconvection gravitactique.

Contents

List of Figures

List of Tables

Nomenclature

A	cavity aspect ratio, $A = L/H$ or $A = R/H$
D_c	cell diffusivity
g	gravitational acceleration
H	cavity height
$\vec{J}$	dimensionless flux of micro-organisms
$\vec{k}$	unit vector
L	cavity width
Le	Lewis number, $Le = \alpha / D_c$
n	dimensionless cell concentration
$\overline{n}$	average cell concentration
$\vec{n}$	unit normal vector to the boundaries
p	dimensionless pressure
Pe	bioconvection Peclet number, $Pe = HV_c / D_c$
q	dimensionless heat flux, $q = \dfrac{\partial T}{\partial z}$
R	cylinder radius
Ra	bioconvection Rayleigh number, $Ra = g\vartheta\Delta\rho\overline{n}H^3 / \rho\nu D_c$
Ra_c	critical bioconvection Rayleigh number
Ra_T	thermal Rayleigh number, $Ra_T = g\beta\Delta TH^3 / \nu\alpha$ or $Ra_T = g\beta qH^4 / \nu\alpha k$

Ra_{Tc} critical thermal Rayleigh number for heating or cooling below

Sc Schmidt number, $Sc = \nu / D_c$

t dimensionless time

T dimensionless temperature

$\vec{u}$ dimensionless fluid velocity

V_c gravitactic cell velocity

(x, y) dimensionless Cartesian coordinate system

(r, z) dimensionless cylindrical coordinate system

Greek symbols

α thermal diffusivity

β volume expansion coefficient

μ dynamic viscosity of the suspension

ν kinematic viscosity of the suspension

ρ_c cell density

ρ_w water density

$\Delta\rho$ difference between cell and water densities, $\Delta\rho = \rho_c - \rho_w$

ϑ cell volume

ψ dimensionless stream function

ω dimensionless vorticity

Superscripts

'	dimensional variable
sub	subcritical
sup	supercritical

Subscripts

max	maximum
min	minimum
ext	extremum

Chapter 1

Introduction

1.1 Objectives

In this master thesis our aim is to study the gravitactic bioconvection of micro-organisms in enclosures. We will investigate bioconvection in a rectangular enclosure with isolated and stress free side walls as shown in Figure 1.1 To examine thermo-bioconvection we consider a vertical cylinder, shown in Figure 1.2, and the effect of heating and cooling from bellow on the bioconvection will be investigated.

Bioconvection is the spontaneous pattern formation in suspensions of micro-organisms, which are little denser than water and move randomly, but on average upwardly against gravity. Up swimming of micro-organisms is generally a response to an external force field such as gravity (gravitaxis or geotaxis), light source (phototaxis), biochemical stimulus such as gradient of oxygen concentration (chemotaxis) and torques due to gravity and shear (gyrotaxis). Due to up swimming, the top layer of the suspension becomes denser than the layer below, resulting in an unstable density distribution. This may lead to a convective instability and formation of convection patterns similar to the patterns observed in the Rayleigh-Bénard convection.

Applications of the bioconvection and thermo-bioconvection are in biotechnology, where various micro-organisms are used. There are also possibilities for the natural exploitation of bioconvection and thermo-bioconvection such as in development of marine life. Bioconvection and thermo-bioconvection by micro-organisms can provide also a unique possibility to better understand various convection phenomena in fluid mechanics and heat transfer, because these systems constitute both the driving force for the convection and the marker particles allowing visualizing the flow. Additionally, appropriate analogies may be discovered to better understand various classical flow phenomena.

1.2 Literature Review

Theoretical models of bioconvection for different types of motile micro-organisms have been developed in various recent publications, including Metcalfe & Pedley [1], Hillesdon & Pedley [2] and Hill et al. [3]. For a review of the fundamental work in this area, see Pedley & Kessler [4] and Hill & Pedley [5].

Rational continuum models for a suspension of purely gravitactic micro-organisms have been formulated and analyzed by Childress et al. [6]. The formulation includes the Navier-Stokes equations with the Boussinesq approximation for an incompressible fluid and the micro-organisms conservation equation. A numerical study based on the equations derived by Childress et al. was presented by Fujita & Watanabe [7]. They discretized the equations using finite difference method with a spatially staggered grid.

They found that the system of bioconvection can lead into chaotic behaviour via a sequence of bifurcations by increasing the Rayleigh number. The preferred wave number of gravitactic bioconvection in a rectangular cavity was studied by Harashima et al. [8] who carried out numerical experiments to show that the system evolves in the direction of intensifying downward advection of micro-organisms and reducing the total potential energy of the system.

Ghorai & Hill [9] studied gyrotactic bioconvection, using a vorticity-stream function formulation of the basic model, which was first introduced by Pedley et al. [10]. The development and instabilities of a single, two-dimensional gyrotactic plume and a periodic array of such plumes were examined in Ghorai & Hill [9] [11]. They investigated numerically the existence and stability of a plume in a suspension of gyrotactic swimming micro-organisms, *C. nivalis*, in a deep and narrow chamber with stress free side walls. Their governing parameters were, in our notation, $Sc = 20$, $Pe = 5$-20, $A = 1$ to 0.125, i.e. square to tall, narrow enclosures. They carried out a parametric study to determine effects of gyrotactic number and cell swimming speed, and the instability mechanism. They carried out also a linear stability analysis at small gyrotactic numbers and found good agreement between the numerical and the linear stability analysis results [9].

Bees and Hill [12] carried out a study by weakly non-linear theory and showed that in gyrotactic swimming micro-organisms in a deep suspension, the bifurcation to instability

was supercritical. They found also that the linear theory was adequate to predict the pattern formation, i.e. the first plumes to appear in an initially well mixed deep suspension of gyrotactic micro-organisms.

The onset of bioconvection and the mechanism of bifurcation are studied by using linear stability theory, nonlinear theory and numerical methods (e.g. [4]). For gravitaxis bioconvection, using weakly nonlinear theory Childress and Spiegel [13] found that the bifurcation in bioconvection of gravitactic micro-organisms in a horizontal fluid layer was subcritical. Alloui et al. [14] studied numerically bioconvection and pattern formation of gravitactic micro-organisms in a vertical cylinder, with the aspect ratio of 1 and 0.1, i.e. square and tall enclosures. They found that the pattern formation at low Peclet numbers was analogous to the Rayleigh-Bénard convection, i.e. the bifurcation was supercritical, while at high Peclet numbers it was subcritical. In contrast, it is found that pattern formation in gyrotaxis bioconvection in tall enclosures was through supercritical bifurcation [9, 12].

Recently, a number of theoretical analyses of thermo-bioconvection of a suspension of gyrotactic and oxytactic micro-organisms have been carried out by Kuznetsov [15-17]. The effect of the temperature gradient on the stability of a suspension of motile gyrotactic micro-organisms in a fluid layer was investigated [15]. It is suggested that this problem may be relevant to motile thermophilic micro-organisms that live in hot springs. The author found that a suspension of gyrotactic micro-organisms in a horizontal fluid layer

heated from below is less stable than the same suspension under isothermal conditions. In a complementary study [15], Nield and Kuznetsov [18] investigated the case where the layer is cooled from below. They presented a linear stability analysis of a suspension of gyrotactic micro-organisms in fluid layer of finite depth. They found that cooling from below stabilizes the suspension and oscillatory convection is possible in certain circumstances. Alloui et al. [19] carried out a linear stability analysis of the thermo-bioconvection in suspension of gravitactic micro-organisms in shallow fluid layers. The effect of heating or cooling from below on the stability was investigated. They found that the thermal effect may stabilize or destabilize the suspension and change the wave length of the bioconvection pattern. In a subsequent study [20], they investigated numerically thermo-bioconvection in a square cavity and found that the bioconvection was stabilized when cooled from below while destabilized by heating below. They observed that there was a transition from subcritical to supercritical when the Rayleigh number was increased.

From the brief review we can see that (a) bioconvection in shallow cavities containing a suspension of gravitactic micro-organisms and the onset and development of bioconvection are not investigated, (b) there are as yet no numerical simulations of thermo-bioconvection flows above the critical Rayleigh numbers in cylindrical cavities, all studies considered only the analytical solutions of the stability problem.

In the first part of this thesis we focus on gravitactic bioconvection developed in a suspension of gravitactic micro-organisms, like *paramecium* and *tetrahymena*, in square to shallow enclosures. The governing parameters are $Sc = 1$, $Pe = 0.1\text{-}10$ and $A = 1\text{-}5$. We will obtain numerical solutions to the governing equations of the continuity, the full Navier-Stokes and the cell concentration at critical conditions for the onset of convection. Our aim is to investigate the effects of the aspect ratio and Peclet number on the onset and development of bioconvection.

In the second part of this thesis we carry out a numerical investigation of the development of thermo-bioconvection in vertical cylinders with stress free sidewalls, which has not been addressed in the literature. We will focus on the effect of heating or cooling from below in case of (i) isothermal and (ii) constant heat flux, and we will investigate the thermal effect of on the bifurcation characteristics of the gravitactic micro-organisms.

This thesis is presented in five chapters. Chapter 1 introduces the bioconvection and contains the problem statement and briefly reviews the previous works done on the subject. In chapter 2 the mathematical model used to solve the problem is described. This chapter includes 3 subchapters; in the first part the numerical model and equations of bioconvection in a rectangular enclosure is derived. In the second part the governing equations for thermo-bioconvection in cylindrical coordinates are given. In the last part the numerical method used to solve the problem is explained. Chapter 3 presents the

results and discussions for the problem of bioconvection in rectangular enclosure. Chapter 4 discusses the results obtained for thermo-bioconvection in a vertical cylinder. Chapter 5 gives the general conclusions of this study.

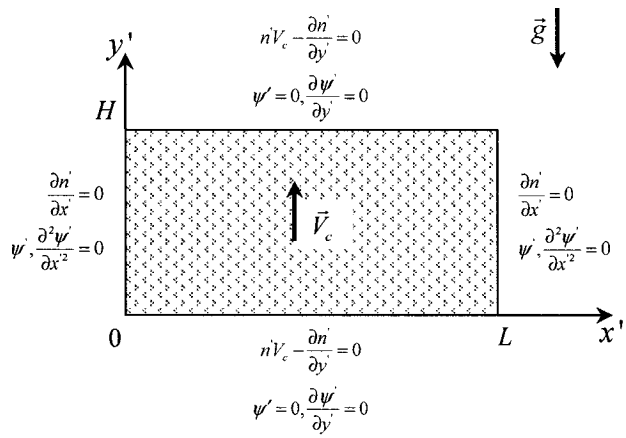

Figure 1.1 Schematic diagram of the computational domain and boundary conditions for bioconvection in rectangular enclosures.

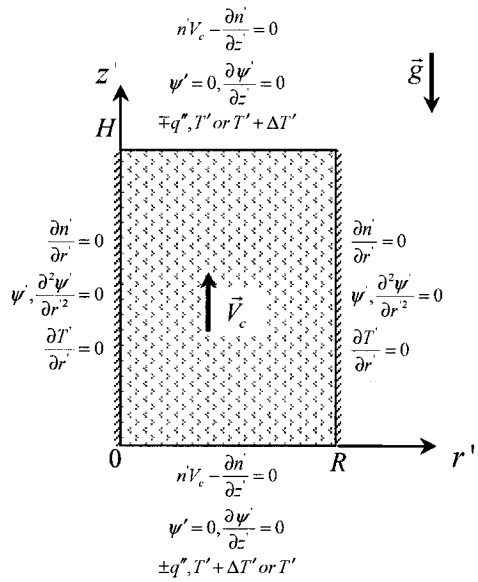

Figure 1.2 Coordinate system, computational domain and boundary conditions for thermo-bioconvection in vertical cylinders.

Chapter 2

Mathematical Models and Numerical Procedure

2.1 Mathematical Model of Bioconvection in Rectangular Enclosures

The system consists of a suspension of gravitactic micro-organisms enclosed in a two-dimensional rectangular cavity of width L and height H referred to Cartesian coordinates (x', y') with the y' axis pointing vertically upwards (Figure 1.1). Initially we have a uniform concentration distribution $\bar{n}$ and each cell has a volume ϑ and density ρ_c. Assuming that the suspension is incompressible and introducing the stream function ψ' and the vorticity ω', we get

$$\vec{u}' = (\partial\psi'/\partial y', -\partial\psi'/\partial x') \tag{1}$$

$$\omega' = -\nabla^2\psi' \tag{2}$$

The Boussinesq approximation assumes that all physical properties are constant except for the density in the buoyancy term, which may be expressed as a linear function of cell concentration

$$\rho = \rho_w + (\rho_c - \rho_w)n'\vartheta = \rho_w(1 + \vartheta\frac{\Delta\rho}{\rho_w}n') \tag{3}$$

where ρ is the density of the suspension, ρ_w and ρ_c the density of the fluid and of the cells, respectively; n' is the number of cells in a unit volume.

The momentum equation under the Boussinesq approximation leads to the vorticity equation

$$\frac{\partial \omega'}{\partial t'} + \nabla.(\omega'\vec{u}') = \nu\nabla^2\omega' - g\vartheta\frac{\Delta\rho}{\rho_w}\frac{\partial n'}{\partial x'} \tag{4}$$

Here ν is the kinematic viscosity of the suspension, which is assumed to be that of the fluid.

The cell concentration can be described by the equation

$$\frac{\partial n'}{\partial t'} = -\nabla.\vec{J}' \tag{5}$$

where the flux of the cells is

$$\vec{J}' = (\vec{u}' + V_c\vec{k})n' - D_c\nabla n' \tag{6}$$

where V_c is the upward velocity, $\vec{k}$ is the vertical unit vector and D_c is the diffusion coefficient of the cells.

We impose rigid, non-slip boundary conditions at the top, bottom and side walls. Also there is no flux of cells through the walls, as shown in Figure 1.1. Hence,

$$\psi' = 0\,,\ \frac{\partial^2 \psi'}{\partial x'^2} = 0 \ \text{ and } \ \vec{J}'.\vec{n} = 0 \qquad \text{at } \ x' = 0, L \tag{7}$$

$$\psi' = 0\,,\ \frac{\partial \psi'}{\partial y'} = 0 \ \text{ and } \ \vec{J}'.\vec{n} = 0 \qquad \text{at } \ y' = 0, H \tag{8}$$

where $\vec{n}$ is the unit vector normal to the boundary.

Length is scaled on the height H, time on the diffusive scale H^2 / D_c, velocity on D_c / H, and the concentration on the mean concentration $\overline{n}$. The resulting system of non-dimensional coupled equations is

$$\omega = -\nabla^2 \psi \tag{9}$$

$$\frac{\partial \omega}{\partial t} + \nabla.(\omega \vec{u}) = Sc\,\nabla^2 \omega - Sc\,Ra \frac{\partial n}{\partial x} \tag{10}$$

$$\frac{\partial n}{\partial t} = -\nabla.\vec{J} \tag{11}$$

where the flux of the cells is

$$\vec{J} = (\vec{u} + Pe\vec{k})n - \nabla n \tag{12}$$

Here $Sc = \nu / D_c$ is the Schmidt number, $Pe = V_c H / D_c$ the bioconvection Peclet number and $Ra = g\vartheta \bar{n} \Delta \rho H^3 / \rho \nu D_c$ the bioconvection Rayleigh number. The Schmidt number is the ratio of momentum diffusivity (viscosity) and mass diffusivity, which is diffusivity of micro-organisms here, and is used to characterize the fluid flow because there is simultaneous momentum and mass diffusion convection processes. The bioconvection Peclet number is the dimensionless number relating the swimming velocity of micro-organisms to the rate of their diffusion. The Rayleigh number describes the relationship between buoyancy of micro-organisms and viscosity forces within the fluid.

The equations (9), (10) and (11) are subjected to the boundary conditions

$$\psi = 0, \frac{\partial^2 \psi}{\partial x^2} = 0 \text{ and } -\frac{\partial \mathrm{n}}{\partial \mathrm{x}} = 0 \text{ at } x = 0, A \tag{13}$$

$$\psi = 0, \frac{\partial \psi}{\partial y} = 0 \text{ and } \mathrm{n\,Pe} -\frac{\partial \mathrm{n}}{\partial \mathrm{y}} = 0 \text{ at } \mathrm{y} = 0,1 \tag{14}$$

where $A = L / H$ is the aspect ratio of the cavity.

2.2 Mathematical Formulation of Thermo-Bioconvection in Vertical Cylinders

The system consists of a suspension of gravitactic micro-organisms enclosed in a cylindrical enclosure of radius R and height H referred to cylindrical Cartesian

coordinates *(r, z)* with the *z* axis pointing vertically upwards. The vertical walls of the enclosure are stress free and the top and bottom walls are rigid. There is no flux of cells through any of the walls. The coordinate system, computational domain and the thermal boundary conditions are shown in Figure 1.2.

We assume that the fluid is incompressible and the flow is axisymmetric. The concentration distribution is uniform and each cell has a volume ϑ and density ρ_c. The two-dimensional Navier-Stokes equations with the Boussinesq approximation, cell conservation equation and energy equation are solved.

$$\nabla.\vec{u}' = 0 \tag{15}$$

$$\rho_w \frac{\partial \vec{u}'}{\partial t'} + \rho_w \nabla.(\vec{u}'\vec{u}') = -\nabla p' + \mu \nabla^2 \vec{u}' + \vartheta \Delta \rho n' \vec{g} - \rho_w \beta (T' - T_0)\vec{g} \tag{16}$$

$$\frac{\partial n'}{\partial t'} = -\nabla \vec{J}' \quad \text{with} \quad \vec{J}' = (\vec{u}' + V_c \vec{k})n' - D_c \nabla n' \tag{17}$$

$$\frac{\partial T'}{\partial t'} + \nabla.(\vec{u}'T') = \alpha \nabla^2 T' \tag{18}$$

By using the vorticity stream function formulation, these equations are made dimensionless using the length scale H, the time scale of H^2/D_c, the velocity scale of D_c / H, the concentration scale $\overline{n}$ and the temperature scale ΔT. The resulting system of coupled equations is

$$\omega = -\nabla^2 \psi \tag{19}$$

$$\frac{\partial \omega}{\partial t} + \frac{\partial (u\omega)}{\partial r} + \frac{\partial (v\omega)}{\partial z} = Sc\left(\nabla^2 \omega - \frac{\omega}{r^2} \right) + Sc\left(Ra \frac{\partial n}{\partial r} - Ra_T Le \frac{\partial T}{\partial r} \right) \tag{20}$$

$$\frac{\partial n}{\partial t} + u\frac{\partial n}{\partial r} + (v + Pe)\frac{\partial n}{\partial z} = \nabla^2 n \tag{21}$$

$$\frac{\partial T}{\partial t} + u\frac{\partial T}{\partial r} + v\frac{\partial T}{\partial z} = Le\nabla^2 T \tag{22}$$

where the governing parameters of the problem are $Sc = \nu / D_c$, the Schmidt number, $Pe = HV_c / D_c$, the bioconvection Peclet number, $Ra = g\vartheta \Delta\rho \bar{n} PeH^3 / \rho \nu D_c$, the bioconvection Rayleigh number, $Ra_T = g\beta \Delta T H^3 / \nu\alpha$ and $Ra_T = g\beta q H^4 / \nu\alpha k$ the thermal Rayleigh numbers, and $Le = \alpha / D_c$, the Lewis number. The physical meanings of the Schmidt, Peclet and bioconvection Rayleigh numbers have been defined earlier. The thermal Rayleigh number is relating buoyancy and viscosity forces within the fluid. The Lewis number is the ratio of thermal diffusivity and diffusivity of micro-organisms.

The computational domain and the boundary conditions are as shown in Figure 1.2. We impose rigid, no-slip boundary conditions at the bottom and top walls and assume that the vertical boundary and the symmetry centerline are stress-free, so that

$$\psi = 0, \frac{\partial \psi}{\partial z} = 0 \qquad \text{at } z = 0,1 \tag{23}$$

$$\psi = 0,\ \frac{\partial^2 \psi}{\partial r^2} = 0 \qquad \text{at } r = 0, A \qquad (24)$$

At the impermeable boundaries, the condition of zero-flux are applied, $\vec{J}.\vec{n} = 0$, i.e.

$$n\,\mathrm{Pe} - \frac{\partial n}{\partial z} = 0 \qquad \text{at } z = 0,1 \qquad (25)$$

$$\frac{\partial n}{\partial r} = 0 \qquad \text{at } r = 0, A \qquad (26)$$

The thermal boundary conditions are isothermal and constant heat flux on horizontal boundaries, and adiabatic at vertical boundary as well as at the symmetry centerline. Hence,

$$T = 1 \text{ or } 0,\ \mathrm{q} = 1 \text{ or } -1 \qquad \text{at } z = 0 \qquad (27)$$

$$T = 0 \text{ or } 1,\ \mathrm{q} = 1 \text{ or } -1 \qquad \text{at } z = 1 \qquad (28)$$

$$\frac{\partial T}{\partial r} = 0 \qquad \text{at } r = 0, A \qquad (29)$$

The initial condition is

$$n = 1,\ T = 0 \qquad \text{at } t = 0 \qquad (30)$$

2.3 Numerical procedure

The control volume method of Patankar [21] is used to discretize governing equations (9)-(12) with a uniform staggered grid with the stream function stored on one set of nodes and the vorticity and concentration stored on another set of nodes. The discretized equations are derived using the central differences for spatial derivatives and backward differences for time derivatives. A line-by-line tridiagonal matrix algorithm with relaxation is used in conjunction with iteration to solve the nonlinear discretized equations.

The validation of the code was done earlier [14], which is summarized here. Eqs. (9) – (11) with Eq. (14) possess a steady state solution with $\psi = \omega = 0$, which is solved analytically and the results are compared to those obtained numerically using the present code. The agreement found was excellent for Pe = 1 and 10. Additionally, by using the present code, we simulated the Rayleigh-Bénard convection in a horizontal fluid layer heated from below by constant temperature and produced the bifurcation diagram. We determined the critical Rayleigh number as 1708, which is consistent with the literature [22].

Uniform grid in x and y direction were used for all computations. Grid convergence was studied for the case of A = 0.5 and Pe = 10 and Ra_T = 0, Ra = 1000, as presented in Table 2.1. Grid sizes were varied from 26x51 to 101x201. Grid independence was achieved

with grid size of 51x101 within 0.3% in extremum stream function with reference to that of 101x201. Similar tests were done with the cavities having A = 1 and 5, and found that the grid size was satisfactory with the following grids: 51x51 for A = 1 and 51x251 for A = 5. The time step Δt was 0.02.

For the case of double diffusion, the code was validated earlier for A = 1.5, Ra_T = 40000, Ra_s = -10^5, Pr = 1, Le = $10^{1/2}$, which showed that the present code reproduced exactly the same iso - patterns of Q, T and S, and very good agreement for $\psi_{\max}$, $\psi_{\min}$, as well as for Nusselt and Sherwood numbers, Nu_m and Sh_m [23].

We consider that the convergence is reached when

$$\frac{\left|f_{i,j}^{k+1} - f_{i,j}^{k}\right|}{\max\left|f_{i,j}^{k}\right|} \leq \varepsilon \tag{31}$$

where f corresponds to the variables (ω, ψ, n) and ε is the prescribed tolerance, k is the iteration number, and i, j denote the grid points. The results were obtained with ε = 10^{-6} and $k = t/\Delta t$ was variable depending on the convergence time t.

Table 2.1 Grid independence study with Ra_T=0, Sc=1, Pe=10 and Ra=10^3

$N_x \times N_y$	26×51	51×101	76×151	101×201
$\psi_{\max}$	0.2861	0.2862	0.2873	0.2870
$n_{\max}$	13.396	11.771	11.580	11.466

Chapter 3

Bioconvection of Gravitactic Micro-Organisms in Rectangular Enclosures

3.1 Introduction

We presented in Chapter 2 the problem description, mathematical model and boundary conditions for this study. The results of this study are submitted for publication [24]. In our computation, we used the following ranges of parameters: Aspect ratio of A = 1, 2 and 5, the bioconvection Peclet number, Pe = 0.1, 1 and 10, the Schmidt number Sc = 1 and the Rayleigh number is variable. Pe and Sc numbers correspond to bioconvection cases with typical micro-organisms (e.g. [25,26]): the diffusion coefficient $D_c = 5\text{x}10^{-3} - 0.5\text{x}10^{-2}$ cm^2/s, the cell velocity $V_c = 7.5\text{x}10^{-3} - 1\text{x}10^{-2}$ cm/s, the cell density $\rho_c = (1.035 - 1.10)\ \rho$, the cell volume $v = 1\text{x}10^{-12} - 5\text{x}10^{-10}$ cm^3, the cell concentration $n = 8.44\text{x}10^5 - 1\text{x}10^9$ cell/cm^3. For example, for *paramecium caudatum* used in [25], $D_c = 5\text{x}10^{-3} - 4.5\text{x}10^{-2}$ cm^2/s, $V_c = 3.2\text{x}10^{-2} - 7.7\text{x}10^{-2}$ cm/s, H = 0.1 cm; we obtain Sc = 0.22 - 2 and Pe = 0.07 - 1.54.

3.2 Results and Discussion

The procedure of determining the critical Rayleigh number and bifurcation was: we begin the simulation with the diffusion state as initial condition, gradually increasing the Rayleigh number until convection arises. The Rayleigh number at which the convection begins corresponds to the supercritical Rayleigh number. We continue to obtain solutions at higher Rayleigh numbers with the solution at the previous, lower Rayleigh number as initial condition. Once the solution at the highest Rayleigh number is obtained, we proceed backward to obtain solutions at lower Rayleigh numbers using the solution at the previous, higher Rayleigh number as initial condition. As Ra is decreased, we continue to obtain solutions until the convection disappears suddenly at a certain value, which corresponds to the subcritical Rayleigh number. Thus, it is found that the bioconvection arises, as the Rayleigh number Ra is increased at a certain *supercritical* value, Ra^{sup}, and disappears suddenly as Ra is decreased at a certain *subcritical* value, Ra^{sub}. It is $Ra^{sub} < Ra^{sup}$. This behaviour is typical of a subcritical bifurcation. It has also been observed experimentally by Mogami et al. [26], who analyzed the temporal and spatial changes in bioconvection pattern with varying gravity. They found a lower threshold, i.e. a lower critical Rayleigh number, for decreasing gravity than for increasing gravity.

We present the results of case with A=1 and Pe=0.1, 1 and 10 in Figure 3.1. For Pe=0.1 in Figure 3.1 (a), we obtain Ra_c^{sub}=16800 and Ra_c^{sup}=20200. Thus, the gravitactic convection is subcritical. This was not the case in cylindrical enclosure in which it was

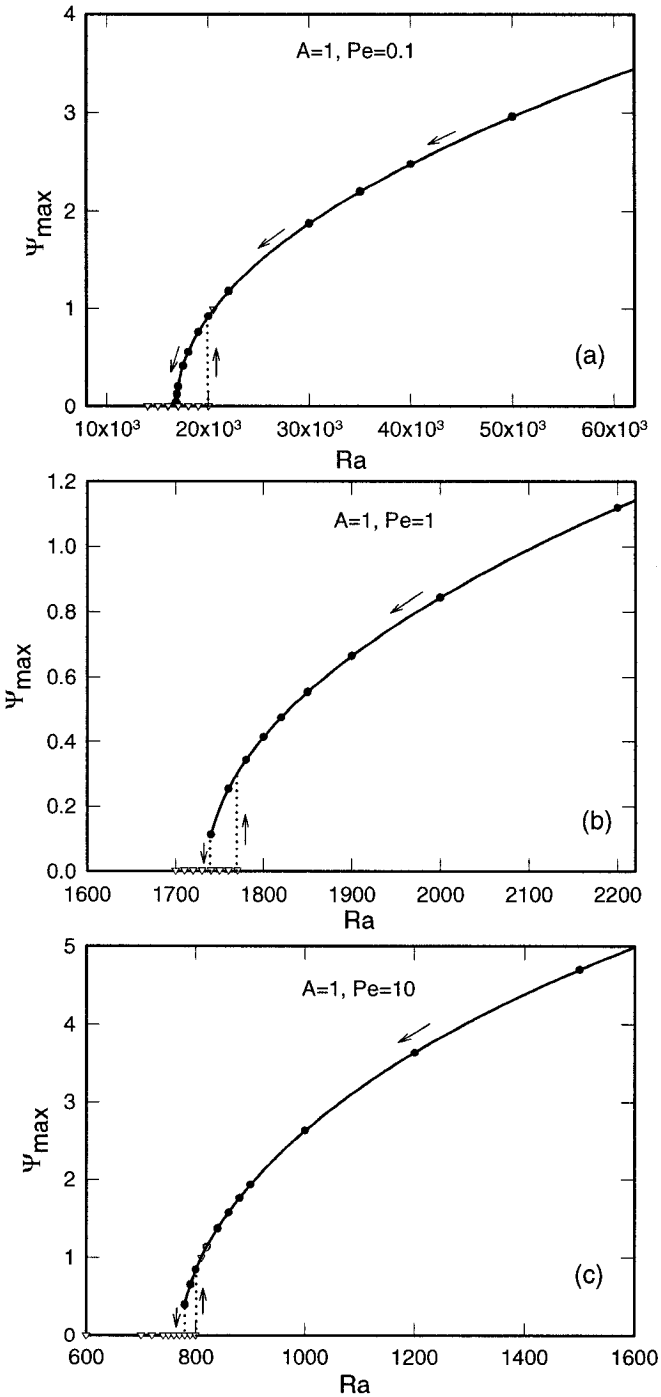

Figure 3.1 Bifurcation diagrams for aspect ratio A=1 and various bioconvection Peclet numbers. (a) Pe=0.1, (b) Pe=1 and (c) Pe=10.

supercritical [14]. For Pe=1 shown in Figure 3.1 (b), it appears that the gravitactic convection is subcritical at Ra_c^{sub}=1730 and its value is reduced considerably by increasing Pe number from 0.1 to 1. We have a supercritical Ra_c^{sup}=1770 from the diffusive state. The solution is unstable as shown in Figure 3.1 (b). When we further increase Pe number to 10, we see in Figure 3.1 (c) that a similar situation is obtained as for Pe=1, i.e. we have a subcritical bifurcation and Ra_c^{sub} is further decreased with increasing bioconvection Pe number. The convection sets in at a supercritical Rayleigh number of Ra_c^{sup} =800, which is obtained from the diffusive state.

We present in Figure 3.2 streamlines and iso-concentration at Rayleigh numbers slightly above the critical Rayleigh number for each case of Figure 3.1, i.e. for Pe=0.1, Ra=17000, Pe=1, Ra=1780 and Pe=10, Ra=780. We see the strong influence of Peclet number on the concentration field: for Pe=0.1, the micro-organism concentration is quasi-uniform in the enclosure, for Pe=1, it is similar to that of Pe=0.1 with some accumulation on the top, and as Peclet is further increased to 10, the micro-organisms are accumulated on the top. The flow patterns show that the fluid flow covers almost all the enclosure regardless of Peclet number.

The results of the case with A=2 and Pe=0.1, 1, 10 are shown in Figure 3.3. We see that the gravitactic convection is subcritical with all three Pe numbers. For Pe=0.1 in Figure 3.3 (a), Ra_c^{sub}=8400, which is smaller than the critical Rayleigh obtained for A=1 for the same Pe number.

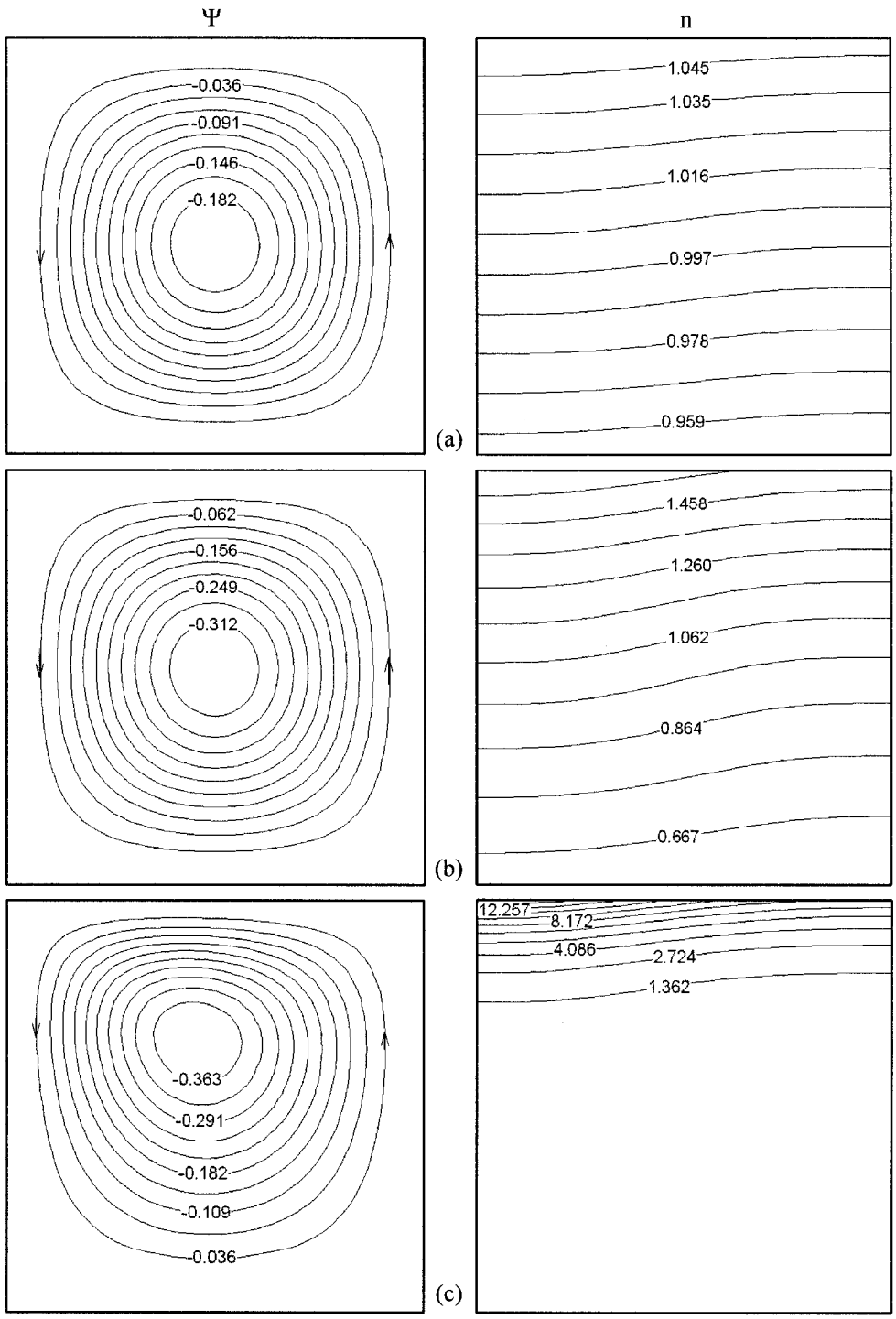

Figure 3.2 Streamlines and iso-concentrations for A=1 of Figure 3.1 (a) Pe=0.1, Ra=17000, (b) Pe=1, Ra=1780, (c) Pe=10, Ra=780.

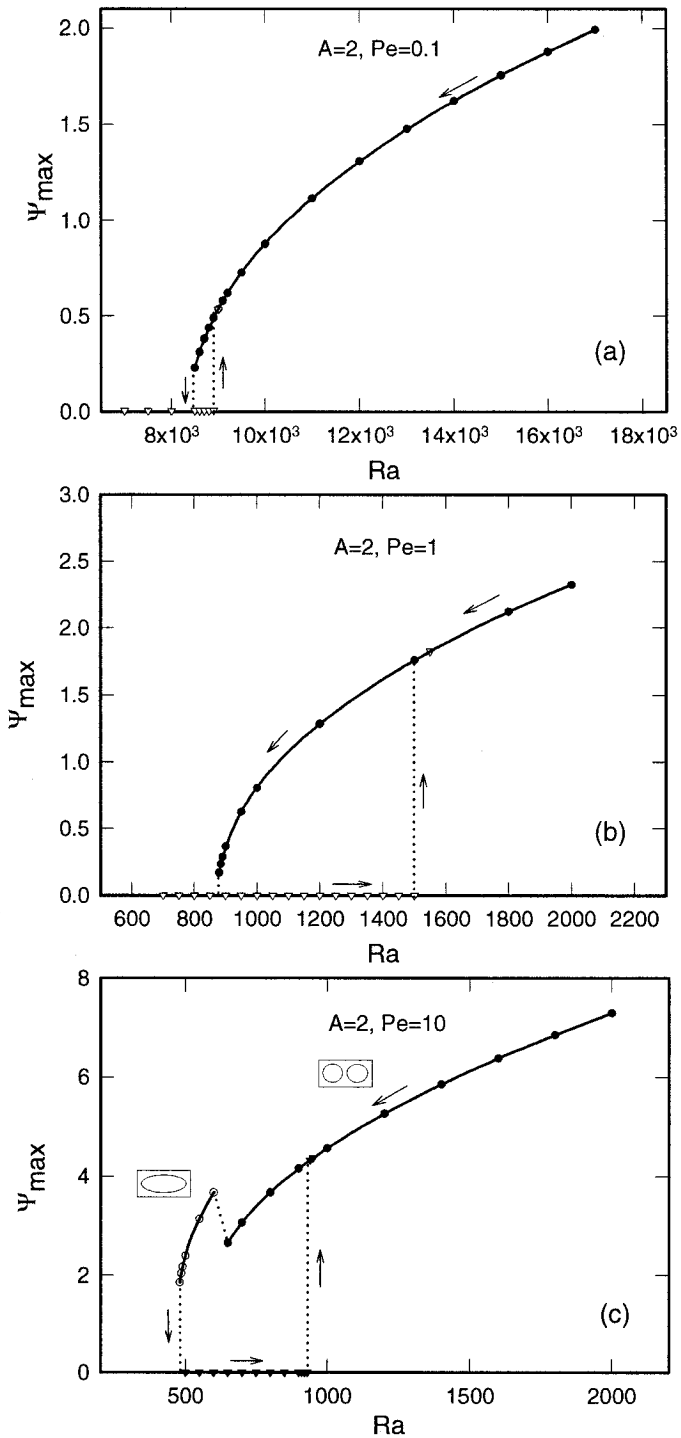

Figure 3.3 Bifurcation diagrams for aspect ratio A=2 and various bioconvection Peclet numbers. (a) Pe=0.1, (b) Pe=1 and (c) Pe=10.

For Pe=1 shown in Figure 3.3 (b), Ra_c^{sub}=870 and for Pe=10 shown in Figure 3.3 (c), Ra_c^{sub}=455. Also in all these cases the critical Rayleigh number is lower than those for the case with A=1. We note that for Pe=10, when the results obtained from the convective state, we have two convection cells from Ra=2000 down to 650 at which the flow field changes to one convection cell. Similarly, in the case of the result obtained from the diffusion state, the supercritical Rayleigh number is 930 at which we get directly a flow field with two convection cells.

We present in Figure 3.4 the flow and concentration fields at Ra=2000, 650 and 600 and for A=2 and Pe=10. At Ra=2000 in Figure 3.4 (a), the flow field is with two convection cells, the left one is clockwise and the right counterclockwise rotating, as a result, the fluid sinks at the center of the enclosure. The micro-organisms are concentrated at the top center. At Ra=650 shown in Figure 3.4 (b), the flow field is similar to the one in Figure 3.4 (a), however with reduced circulation strength. As a result, we have a similar iso-concentration pattern. At Ra=600 in Figure 3.4 (c), we have a single counterclockwise circulating convection cell at the left upper corner and the micro-organisms form a layer at that corner.

We present the shallow enclosure case, A=5 with Pe from 0.1 to 10 in Figure 3.5. For Pe=0.1 in Figure 3.5 (a) we have a subcritical bifurcation at Ra_c^{sub}=6990. The gravitactic convection obtained from the convection state is with the flow field having four

convection cells from $Ra \sim 50x10^3$ down to 13000, then the flow field becomes one with two convection cells, for Ra from 12000 down to 6990. By continuing at lower Ra numbers, the convection disappears suddenly at 6990. Starting with diffusive state, we obtain the supercritical Rayleigh number, Ra_c^{sup}=9600, slightly above which, the gravitactic convection begins with two convection cells.

For Pe=1 shown in Figure 3.5 (b), we have a subcritical bifurcation. The gravitactic convection obtained from the convection state is with four cells. By continuing at lower Rayleigh numbers, the flow with three cells is obtained at Rayleigh about 1200 down to

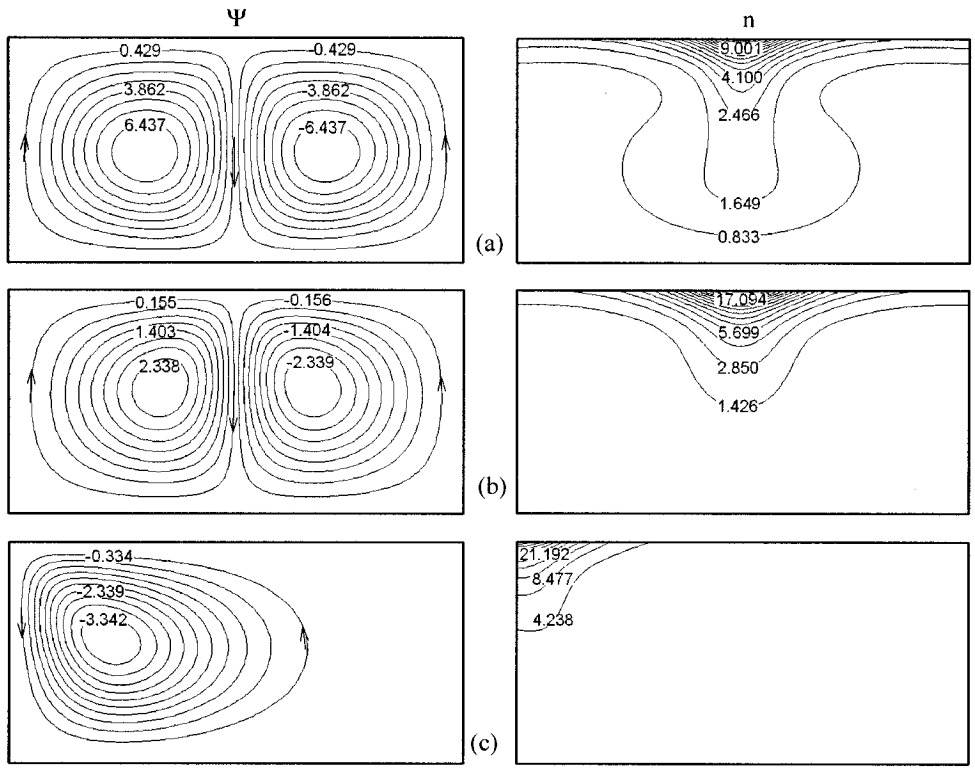

Figure 3.4 Iso-lines for A=2 and Pe=10 of bifurcation diagram in Figure 3.3(c) at various Rayleigh numbers. (a) Ra=600, (b) Ra=650 and (c) Ra=2000. Streamlines are shown on the left and iso-concentration on the right.

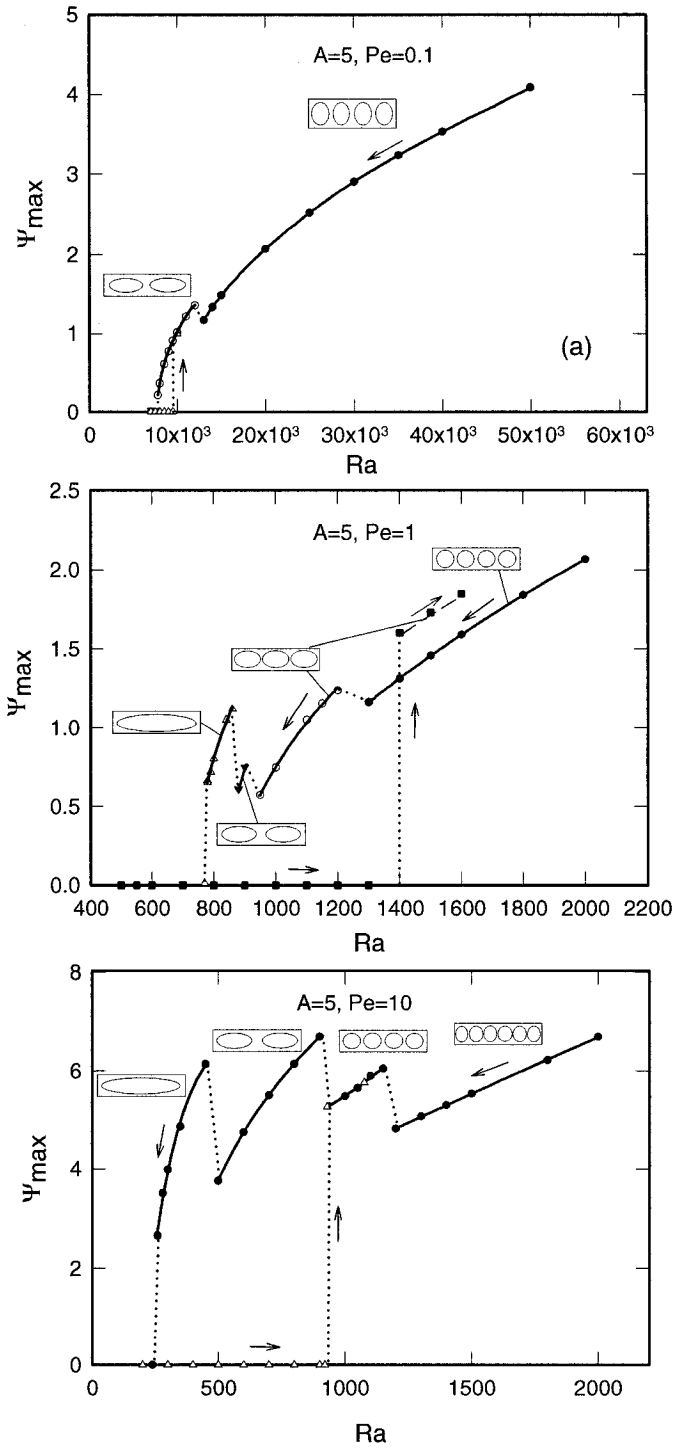

Figure 3.5 Bifurcation diagrams for aspect ratio A=5 and various bioconvection Peclet numbers. (a) Pe=0.1, (b) Pe=1 and (c) Pe=10.

950. Then, the flow becomes with two cells at Ra=905. By continuing still at lower Ra numbers, the two cells convection becomes one cell convection at Ra=870. Then, the convection disappears at Rayleigh number, Ra_c^{sub}=775. Starting from the diffusive state, we have a supercritical Rayleigh number at Ra_c^{sup}=1450, above which we obtain convection with three convection cells, yet at the same Rayleigh number, we obtained four convection cells in case of starting from the convection state. As discussed before, this is due to unstable convective flow.

To see these different states, we plotted streamlines and iso-concentration, and presented in Figure 3.6 to illustrate the flow and concentration fields thus obtained corresponding to various states observed in Figure 3.5 (b). For Ra=2000 shown in Figure 3.6 (a), we see four convection cells and the concentration varies in a way corresponding to the cells formed. The left convection cell is counterclockwise, the next two convection cells in the central part are clockwise and counterclockwise circulating and the last convection cell at the right is clockwise circulating. Thus, the micro-organisms are concentrated on the top at the left and right corners and at the center above the two convection cells in the center. For Ra=1200 in Figure 3.6 (b), we have three convection cells formed. The right convection cell is clockwise circulating as a result of which the micro-organisms are concentrated on the top at the right corner. As the center convection cell circulating counterclockwise and the left one clockwise, they are concentrated on top of the two left cells. At Ra=900 in Figure 3.6(c), we see the micro-organisms are concentrated at the top corners corresponding to counterclockwise circulating left convection cell and clockwise

circulating right convection cell. At Ra=780 in Figure 3.6 (d) we have a flow with single counter clockwise circulating convection cell squeezed to the right, the micro-organisms are concentrated at the top right corner.

As *Pe* increased to 10, shown in Figure 3.5 (c), the bifurcation is subcritical at Ra_c^{sub}=250. The solution obtained from the convection state is with six convection cells. By continuing at lower Rayleigh numbers, the flow with four convection cells is obtained at Rayleigh about 1150 down to 920, and then with two convection cells at 900 down to 505. At still lower Ra numbers, the convection becomes single cell at 450 and it disappears at Ra_c^{sub}=250. Starting from the diffusive state, the bifurcation is supercritical at Ra_c^{sup}=920, above which we obtain convection with four convection cells. The influence of Peclet number at various Rayleigh numbers in this case is shown in Figure 3.7. At *Ra*=1500 in Figure 3.7 (a), the flow field is with six convection cells and the iso-concentration

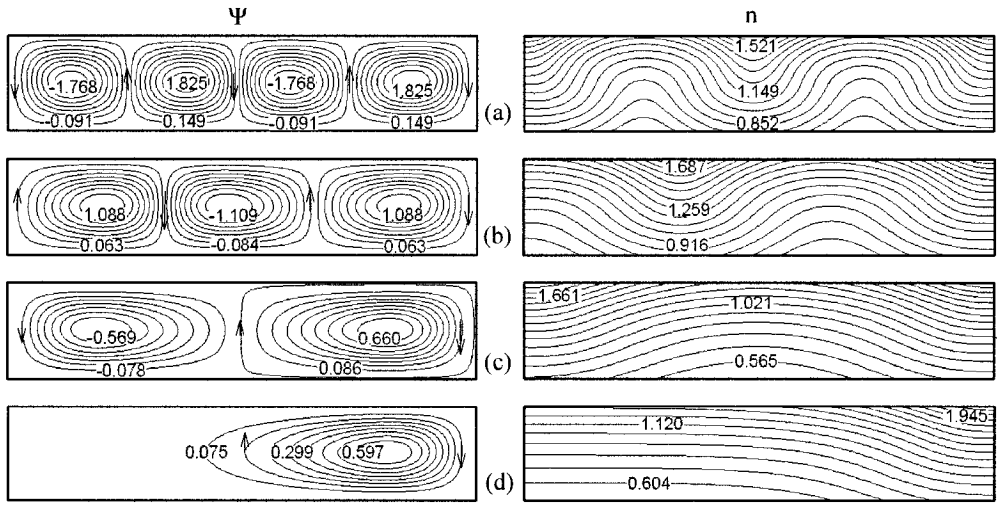

Figure 3.6 Iso-lines for A=5 and Pe=1 of bifurcation diagram in Figure 3.5(b) at various Rayleigh numbers. (a) *Ra*=2000, (b) *Ra*=1200, (c) *Ra*=900 and (d) *Ra*=780. Streamlines are shown on the left and iso-concentration on the right.

follows the pattern of each pair of convection cells: the micro-organisms are accumulated at the top location corresponding to the sinking fluid of each pair. At Ra=1000 in Figure 3.7 (b), the flow field is with four convection cells. The left and right cells rotate counterclockwise and clockwise respectively and as a result, the micro-organisms are accumulated at the left and right corners at the top. At the center, the fluid sinks by the counterclockwise and clockwise rotating pair of convection cells and we see the micro-organisms are accumulated at the top center. At Ra=700 in Figure 3.7 (c), there are two convection cells, the left one counterclockwise and the right one clockwise rotating. The micro-organisms are accumulated at the top corners. At Ra=300 in Figure 3.7 (d), just above Ra_c^{sub}, the flow field becomes with a clockwise rotating single convection cell and the micro-organisms are accumulated at the right corner.

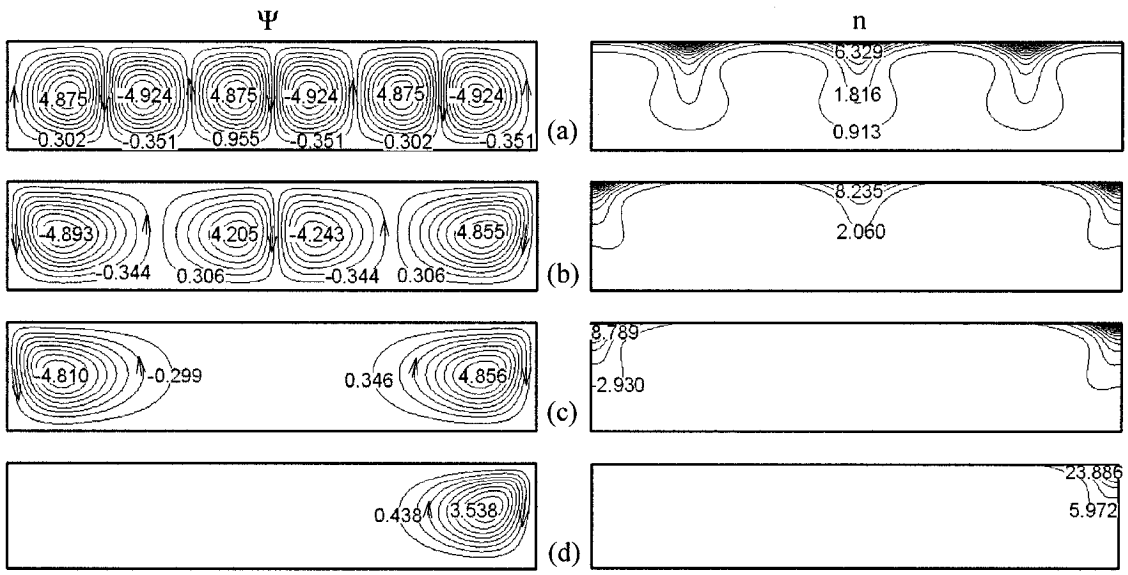

Figure 3.7 Streamline and iso-concentration patterns at various Rayleigh numbers of Figure 3.5(c) for A=5, Pe=10. (a) Ra=1500, (b) Ra=1000, (c) Ra=700, (d) Ra=300.

For Pe = 1 and 10 in Figure 3.5 (b) and (c), the convective flow in the region between Ra_c^{sup} and Ra_c^{sub} is unstable where, depending on the Rayleigh number, different convection patterns are formed. In fact, we see in Figure 3.5 (b) and (c) and the corresponding patterns in Figure 3.7 that the number of convection cells formed changes from 4 to 2 and from 2 to 1 before reaching the subcritical Rayleigh number.

To see the mechanism of pattern change near the supercritical Rayleigh number of Figure 3.5 (c), we present the time sequence diagrams at Ra = 1000, 900 and 800 in Figure 3.8. Following the procedure explained earlier, we obtained the solution at Ra = 1000 by using the solution from the previous solution at Ra = 1050 from which we get (t = 0.02, ψ_{ext} = 5.634). We see in Figure 3.8 (a) that after a relatively short computation time (t = 0.75, ψ_{ext} = 5.542), the solution becomes quasi steady-state, a typical time sequence. After satisfying the convergence criteria Eq. (31), we obtain (t = 12.26, ψ_{ext} = 5.5424, Ra = 1000), which is on the bifurcation curve with four convection cells. To obtain solution at Ra = 900 < Ra_c^{sup} = 920, we follow the same procedure and use the solution at Ra = 1000. The time sequence diagram is shown in Figure 3.8 (b); in a very short computation time at (t = 0.02, ψ_{ext} = 5.3202), ψ_{ext} increases steadily from (t = 0.30, ψ_{ext} = 5.0108) to (t = 762, ψ_{ext} = 5.6219), and then it increases suddenly to (t = 768, ψ_{ext} = 6.6725) and finally a converged solution is obtained at (t = 833, ψ_{ext} = 6.6935, Ra = 900), at which we have a pattern of two convection cells. The next computation at lower Ra = 800 is done similarly by reading the solution from Ra = 900, the time sequence diagram of which is shown in Figure 3.8 (c). We observe that the time sequence is once more a typical one, like in

Figure 3.8 (a), and the solution is (t = 12.54, ψ_{ext} = 6.1363, Ra = 800) with two convection cells. We note that the mechanism of pattern formation observed here is quite different from that of gyrotactic bioconvection in narrow and tall enclosures [9].

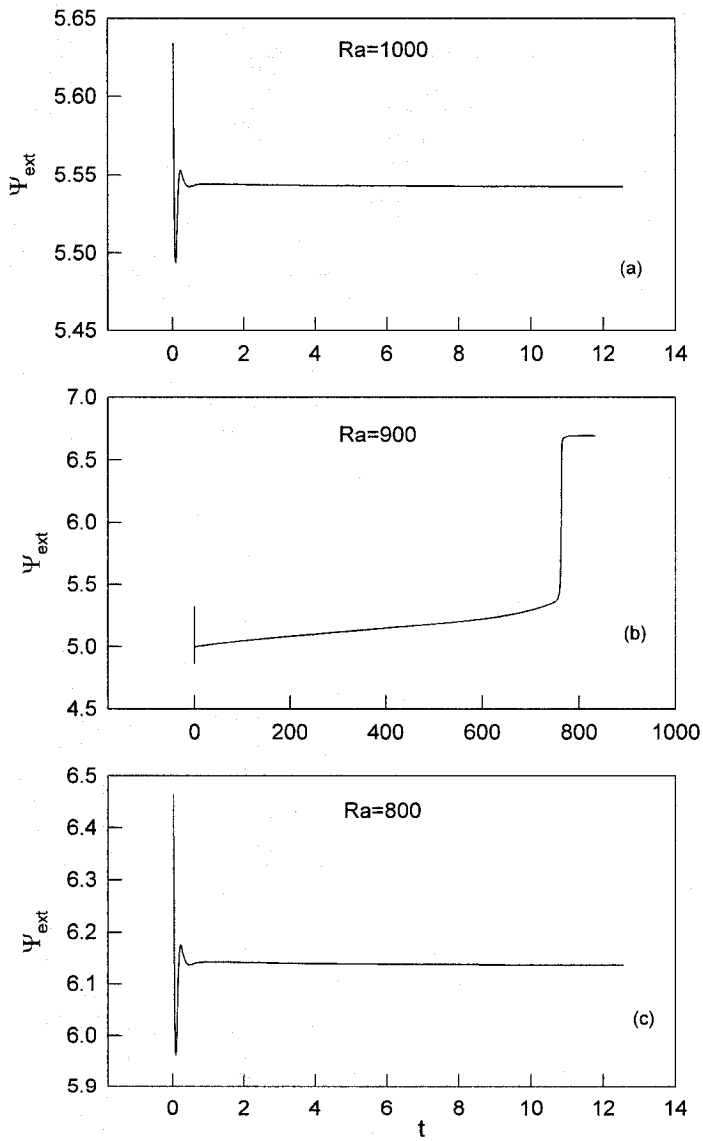

Figure 3.8 Time sequence diagrams corresponding to the case with A=5, Pe=10 of Figure 3.5(c) at a) Ra =1000, b) Ra = 900, c) Ra = 800.

3.3 Conclusion

Numerical simulations of gravitactic bioconvection in rectangular enclosures were carried out. The vertical walls of the cavity are assumed to be stress-free and insulated, while horizontal boundaries are rigid. The governing equations are integrated numerically using the control volume method. The present results exhibit the influence of bioconvection Peclet number and aspect ratio on the bifurcation diagram and the flow structure. We have found that the bifurcation remains subcritical in all cases when the bioconvection *Pe* number is varied from 0.1 to 10 in rectangular enclosures having an aspect ratio from 1 to 5.

Chapter 4

Thermo-Bioconvection of Gravitactic Micro-Organisms in Vertical Cylinders

4.1 Introduction

In this chapter we investigate the effect of heating or cooling from below at constant temperature and constant heat flux on the development of gravitactic bioconvection in vertical cylinders with stress free sidewalls. The mathematical model and boundary conditions are presented in section 2.3. Computations were performed with the aspect ratio of A = 1, 0.5, 0.2 and variable Ra_T and Ra for the following values of dimensionless parameters: $Sc = 1$, $Le = 1$, Pe = 1 and 10, which correspond to typical bioconvection cases with known micro-organism characteristics (e.g. [25-26]), First, we obtained bifurcation curves by numerical simulation, the critical thermal Rayleigh numbers, Ra_{Tc} without bioconvection, i.e. with Ra = 0. Then, we obtained bifurcation curves by numerical simulation, and the subcritical bioconvection Rayleigh numbers, Ra_c without thermal effect, i.e. with Ra_T = 0. Finally, by using the critical thermal Rayleigh numbers and the subcritical bioconvection Rayleigh numbers, we carried out numerical simulation to obtain bifurcation curves to determine the critical Rayleigh numbers at Ra_T = 1xRa_{Tc}, 2xRa_{Tc} (i.e. heating from below) and Ra_T = -1xRa_{Tc}, -2xRa_{Tc} (i.e. cooling from below) using the conditions of T = constant and q = constant.

4.2 Results and discussion

Figure 4.1 displays the bifurcation diagrams ($\psi_{\max}$ vs. Ra_T) for the case of thermal convection, i.e. no bioconvection, $Ra = 0$, for heating from the bottom at isothermal and constant heat flux. A bifurcation between purely conductive and convective states is clearly seen in Figure 4.1 (a), (b) and (c) at Ra_{Tc} = 2,265, 10,800 and 299.4x10^3 for A = 1, 0.5 and 0.2 respectively. They are the critical Rayleigh numbers of a horizontal fluid layer in a vertical cylinder heated from below at constant temperature. Similarly we see in Figure 4.1 (d), (e) and (f) the bifurcations at Ra_{Tc} = 1,708, 10,350 and 298x10^3, which are the critical Rayleigh numbers when heated from below at constant heat flux. The situations in Figure 4.1 (a)-(c) correspond to the classical Rayleigh-Bénard problem [27].

Figure 4.2 shows the bifurcation diagrams (ψ_{ext} vs. Ra) for the case of isothermal cavity i.e. at Ra_T = 0. These results are obtained by beginning the simulation at a high Rayleigh number, which is estimated by trial and error to have a convection state. We obtained solutions at lower Rayleigh numbers using the solution at the previous (higher) Rayleigh number as initial condition. Then, we started with the diffusion state (i.e. no convection) as initial condition, gradually increasing the Rayleigh number until convection arose. As usual, at each step we continued to obtain solutions at higher Rayleigh numbers by initializing using the solution at the previous (lower) Rayleigh number. Thus, we determined the supercritical Rayleigh numbers.

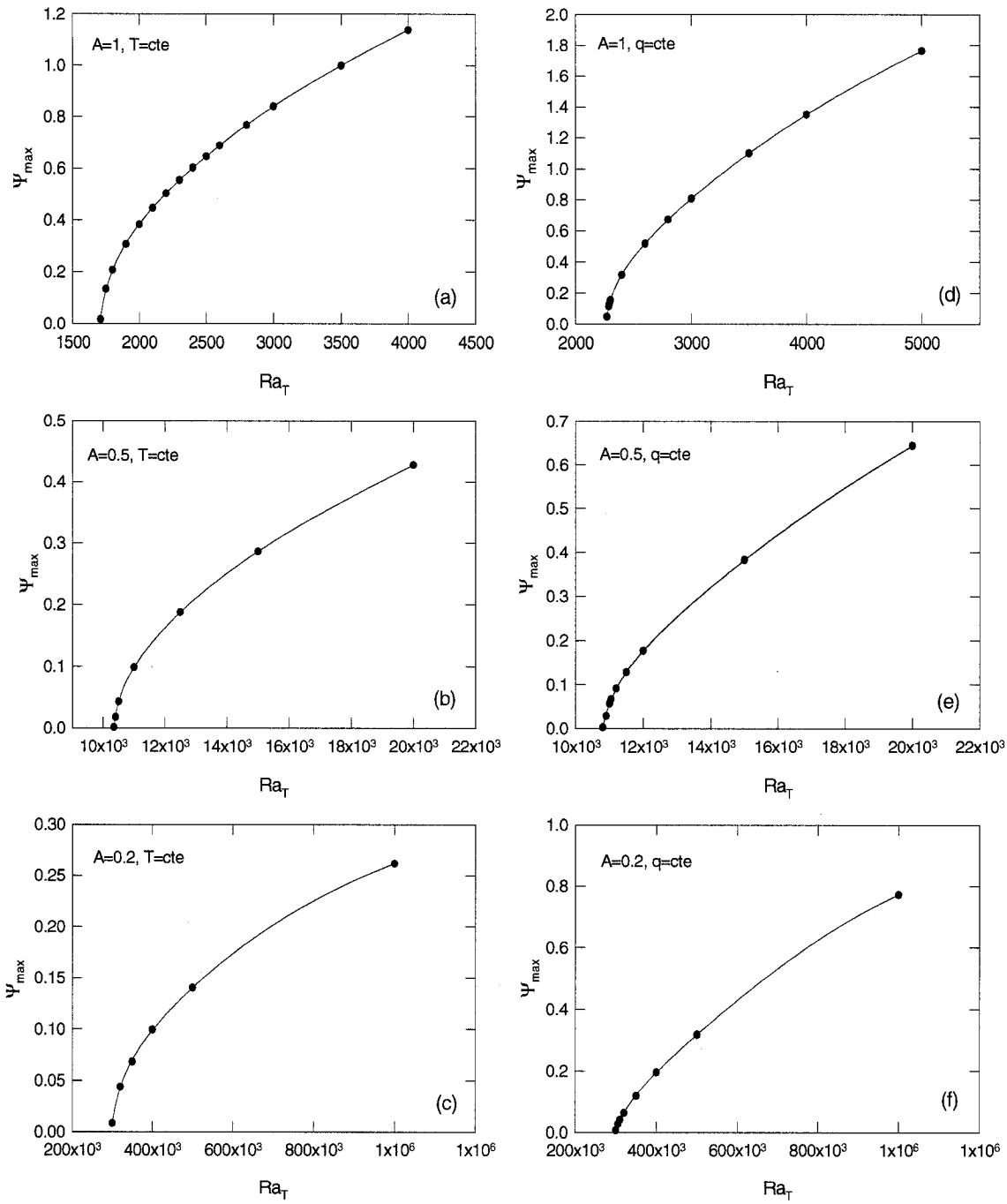

Figure 4.1 Bifurcation diagram for Ra=0 (no bioconvection). (a) A=1, T=constant, (b) A=0.5, T=constant, (c) A=0.2, T=constant, (d) A=1, q=constant, (e) A=0.5, q=constant, (f) q=0.2, q=constant.

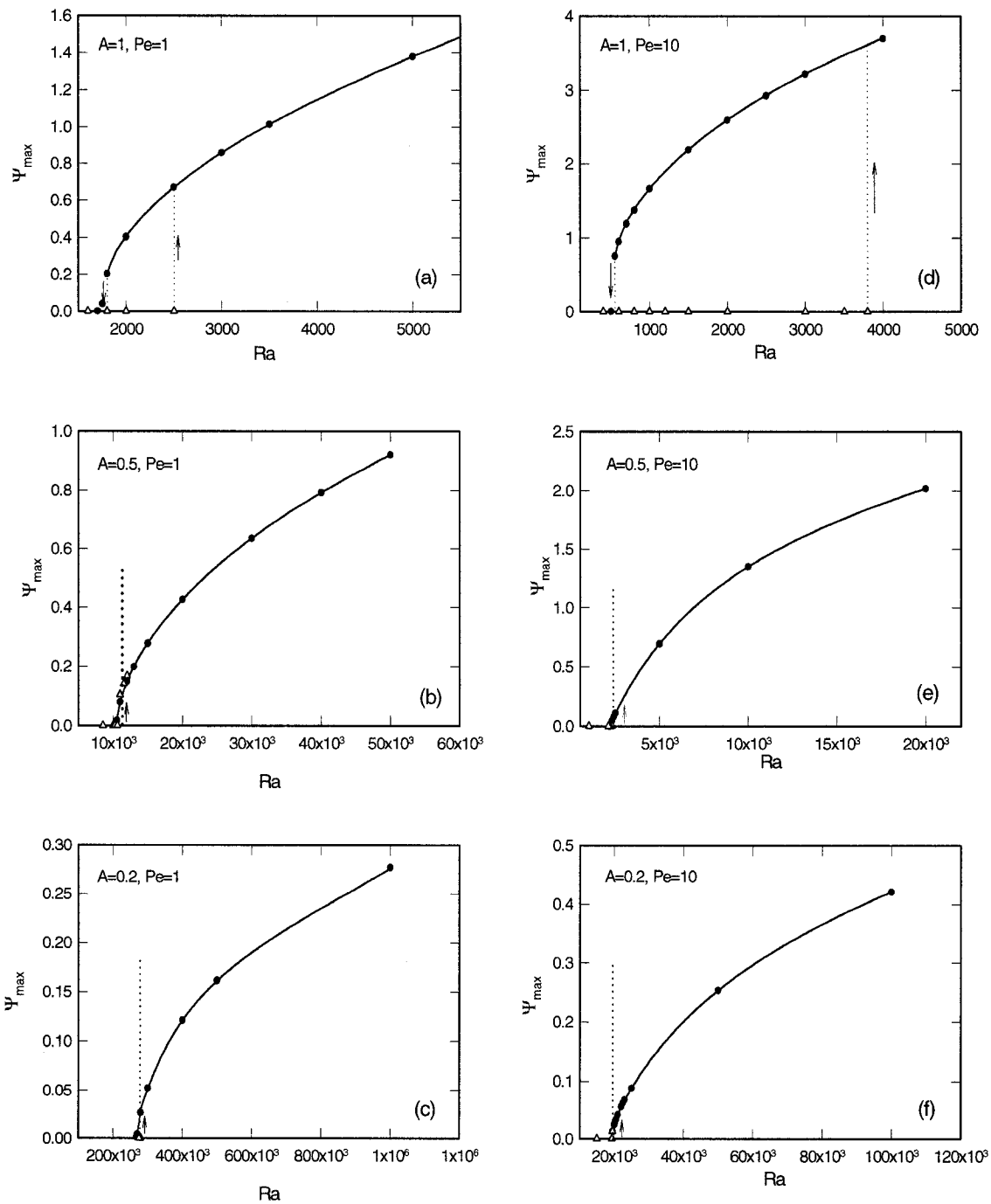

Figure 4.2 Bifurcation diagram for Ra_T =0 (no thermal effect). (a) A=1, Pe=1, (b) A=0.5, Pe=1, (c) A=0.2, Pe=1, (d) A=1, Pe=10, (e) A=0.5, Pe=10, (f) A=0.2, Pe=10.

We see that the bifurcations are all subcritical with bioconvection Rayleigh numbers, Ra_c^{sub}, which are obtained for the cases of a horizontal fluid layer in a vertical cylinder for Pe = 1 in Figure 4.2 (a)-(c) and for Pe = 10 in Figure 4.2 (d)-(f). The subcritical bioconvection Rayleigh numbers for Pe = 1 are Ra_c^{sub} = 1,710, 10,400 and 270x10^3 for A = 1, 0.5 and 0.2 respectively. For Pe = 10, they are Ra_c^{sub} = 520, 2,160 and 19,000 for A = 1, 0.5 and 0.2 respectively. We note that the subcritical bioconvection Rayleigh number is higher for smaller bioconvection Peclet number, i.e. for a given bioconvection Rayleigh number; the bioconvection strength is higher at higher Peclet number. The same phenomenon was also observed earlier [28]. We note also that for the aspect ratio of A = 1, the unstable region between Ra_c^{sub} and Ra_c^{sup} is quite distinct. Yet, for A = 0.5 and 0.2 it is almost merged. For example, for A = 0.5 and Pe =1, Ra_c^{sub} =10,400 and Ra_c^{sup} = 11,000 and for A = 0.5 and Pe =10, Ra_c^{sub} =2,160 and Ra_c^{sup} = 2,350; for A = 0.2 and Pe =1, Ra_c^{sub} =269,000 and Ra_c^{sup} = 280,000 and for A = 0.2 and Pe =10, Ra_c^{sub} =19,100 and Ra_c^{sup} = 19,500.

We studied the effect of heating and cooling from below at constant temperature and constant heat flux with the bioconvection Peclet number of 1 and 10, and the aspect ratio of A = 1, 0.5 and 0.2. We obtained bifurcation diagrams with Ra_T = 1xRa_{Tc} and 2xRa_{Tc} (i.e. corresponding to heating from below) and Ra_T = -1xRa_{Tc} and -2xRa_{Tc} (i.e. corresponding to cooling from below) at constant temperature and constant heat flux; the critical thermal Rayleigh numbers employed here, Ra_{Tc} are those obtained for heating

from below at constant temperature and constant heat flux and presented in Figure 4.1. The procedure we followed was to use a starting Rayleigh number, $Ra \geq 5\text{x}Ra_c$ and after obtaining the first solution, continue to obtain a new solution at a lower Ra by using the previous solution at higher Ra as initial condition. We continued the same procedure until we obtained diffusive state.

Bifurcation results are shown in Figure 4.3 (a-c) for $Pe = 1$ and Figure 4.4 (a-c) for $Pe = 10$ respectively. Each figure shows the bifurcation diagrams for heating and cooling from below with constant temperature (shown with dashed lines) and constant heat flux (shown with full lines) for $A = 1$, 0.5 and 0.2 in figures (a), (b) and (c) respectively. In addition, the bifurcation curve for $Ra_T = 0$, i.e. the bioconvection bifurcation curve for a given A is also included in the same figure for the same A as reference.

Generally, in all bifurcations the extremum stream function ψ_{ext} is smaller at a given Rayleigh number when the fluid layer is cooled from below by a constant temperature or constant heat flux with respect to that of the bioconvection only. Thus, we see in Figure 4.3 (a-c) that the bifurcation diagrams fall below the bioconvection bifurcation diagram and the critical Rayleigh numbers are higher. This case represents opposing buoyancy forces and the resulting convection is reduced. In general, we see that the convection is reduced more when the cooling from below is by a constant temperature. Another striking result is that the critical Rayleigh numbers obtained by cooling from below by constant temperature and constant heat flux are the same.

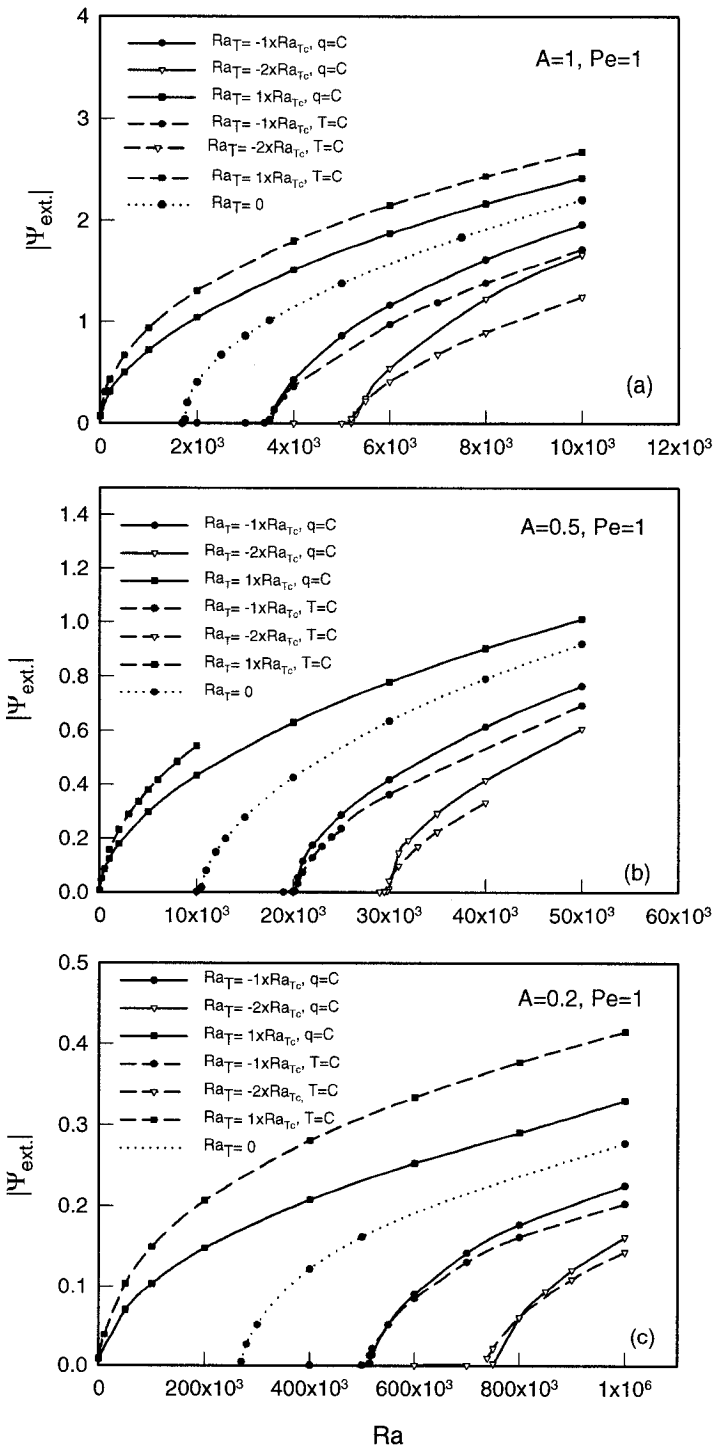

Figure 4.3 Bifurcation diagram for Ra_T = -1x Ra_{Tc}, -2x Ra_{Tc}, 1x Ra_{Tc} and Pe=1. (a) A=1, (b) A=0.5, (c) A=0.2.

In contrast, the extremum stream function ψ_{ext} at a given Rayleigh number is higher than that of bioconvection when the fluid layer is heated from below. This case corresponds to cooperating buoyancy forces and the resulting convection is enhanced. The convection is higher when heated from below at constant temperature than at constant heat flux. Similar to the case of cooling from below, the critical Rayleigh numbers for this case with $Ra_T = 1 \times Ra_{Tc}$ for heating at constant temperature and constant heat flux are the same and equal to zero, as they should be, since $Ra_T = Ra_{Tc}$ as found earlier. However, at $Ra_T = 2 \times Ra_{Tc}$ we could not obtain critical Rayleigh numbers, hence no bifurcation. Indeed, for this case of heating at constant temperature and constant heat flux, we checked starting from diffusion state, i.e. initializing at uniform temperature and concentration and obtained convection only. This shows that the cooperating thermal buoyancy forces are too strong and a diffusion state does not exist. We present ψ_{ext} obtained at $Ra = 0$ and its coordinates in Table 4.1 for the case of $Ra_T = 2 \times Ra_{Tc}$; i.e. heating from below at constant temperature and at constant heat flux, and for various aspect ratios. We see in this table that $\psi_{ext}(r,z)$ is exactly the same for Pe=1 and 10 and for each aspect ratio. The iso-lines for ψ_{ext}, n and T showed that for $A = 1$ and 0.5, there was a single clockwise rotating convection cell. The isotherms and iso-concentration lines (not presented here) showed similar trends with micro-organisms concentration near the top corner at $r = A$ when heated from below at constant heat flux and with micro-organisms concentration at the center, r=0 when heated from below at constant temperature. We note that at $Ra = 0$, there is no bioconvection and the concentration of

Table 4.1 ψ_{ext} and its coordinates for Ra_T=2xRa_{Tc} at Ra=0

Aspect Ratio, A	Pe	Thermal boundary condition	Ra_T	Ψ_{ext}	(r,z)
1	1	q=const.	2x1710	0.9821	(0.58,0.56)
		T=const.	2x2270	1.5893	(0.58,0.42)
	10	q=const.	2x1710	0.9821	(0.58,0.56)
		T=const.	2x2270	1.5893	(0.58,0.42)
0.5	1	q=const.	2x10350	0.4450	(0.28,0.34)
		T=const.	2x10800	0.6489	(0.28,0.32)
	10	q=const.	2x10350	0.4450	(0.28,0.34)
		T=const.	2x10800	0.6489	(0.28,0.32)
0.2	1	q=const.	2x298000	0.1466	(0.11,0.845)
		T=const.	2x299400	0.4306	(0.11,0.135)
	10	q=const.	2x298000	0.1466	(0.11,0.845)
		T=const.	2x299400	0.4306	(0.11,0.135)

micro-organisms at the top is as a result of thermal convection. For A = 0.2, similar observation was made when heated from below at constant temperature but there were two symmetrical convection cells with respect to mid-plane when heated from below at constant heat flux. Consequently, isotherms and iso-concentration lines were also similarly symmetric with respect to mid-plane. We see in Figure 4.3 (a-c) that the effect of increasing aspect ratio on the critical Rayleigh number is to decrease it.

We see in Figure 4.4 (a-c) that the effect of heating and cooling from below is relatively higher for Pe = 10 than for Pe = 1 since the strength of the bioconvection is relatively higher in the former case. The reason is that Pe is non-dimensional swimming velocity of micro-organisms in opposing direction to the gravity and thermal diffusion forces in case of cooling from below. It is in the same direction in case of heating from below. Thus, we will have opposing forces in play in case of cooling from below and cooperating forces in case of heating from below. Indeed, we see in Figure 4.4 (a-c) that as expected, with all

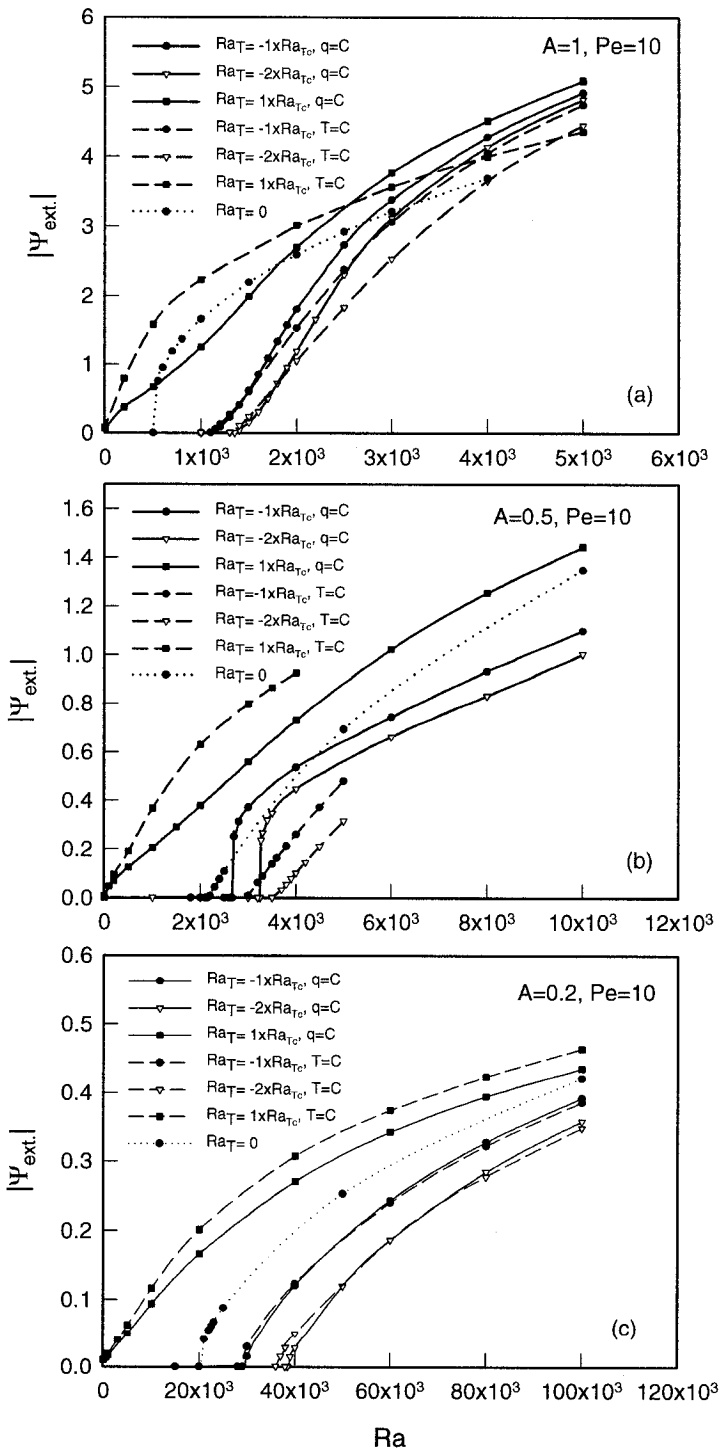

Figure 4.4 Bifurcation diagram for Ra_T = -1x Ra_{Tc}, -2x Ra_{Tc}, 1x Ra_{Tc} and Pe=10. (a) A=1, (b) A=0.5, (c) A=0.2.

three aspect ratios $Ra_{Tc} = 0$ at $Ra = 0$ for $Ra_T = 1xRa_{Tc}$. Generally, for the opposing buoyancy case, i.e. cooling from below, convection is lower than that for bioconvection only, i.e. $Ra_T = 0$. It is the reverse in the cooperating buoyancy case, i.e. heating from below. In case with $Ra_T = 2xRa_{Tc}$ in heating from below at constant temperature and constant flux, we observed the same phenomenon of sudden convection starting from diffusion state at $Ra = 0$. For this case ψ_{ext} obtained at $Ra = 0$ and its coordinates are also shown in Table 4.1. We see that ψ_{ext} and their coordinates are the same as for $Pe = 1$. The reason, as discussed before, is because there is no bioconvection at $Ra = 0$. By examining the iso-lines for this case we noticed that they were all identical to those for $Pe = 1$ except iso-concentration lines. They showed almost total accumulation of micro-organisms at the top right corner near $r = A$ when heated from below at constant heat flux and at the center $r = 0$ when heated from below at constant temperature. We see in Figure 4.4 (a) and (c) that in case of $A = 1$ and 0.2, as observed earlier with $Pe = 1$ in Figure 4.3, the critical Rayleigh numbers are the same or almost the same for cooling from below at constant temperature and at constant heat flux. However, they are not the same in case of $A = 0.5$ in Figure 4.4 (b). In this case, the critical Rayleigh number is higher for cooling from below at constant temperature than at constant heat flux.

To see the reason we produced iso-lines Ψ, n, T at near critical Rayleigh numbers for the cases of constant temperature and heat flux, all for cooling from below and presented in Figure 4.5. For the case with $Ra_T = -1xRa_{Tc}$, and $Ra = 3{,}000$ and 2,700 for constant temperature or heat flux respectively, we find that all three iso-lines are quite different:

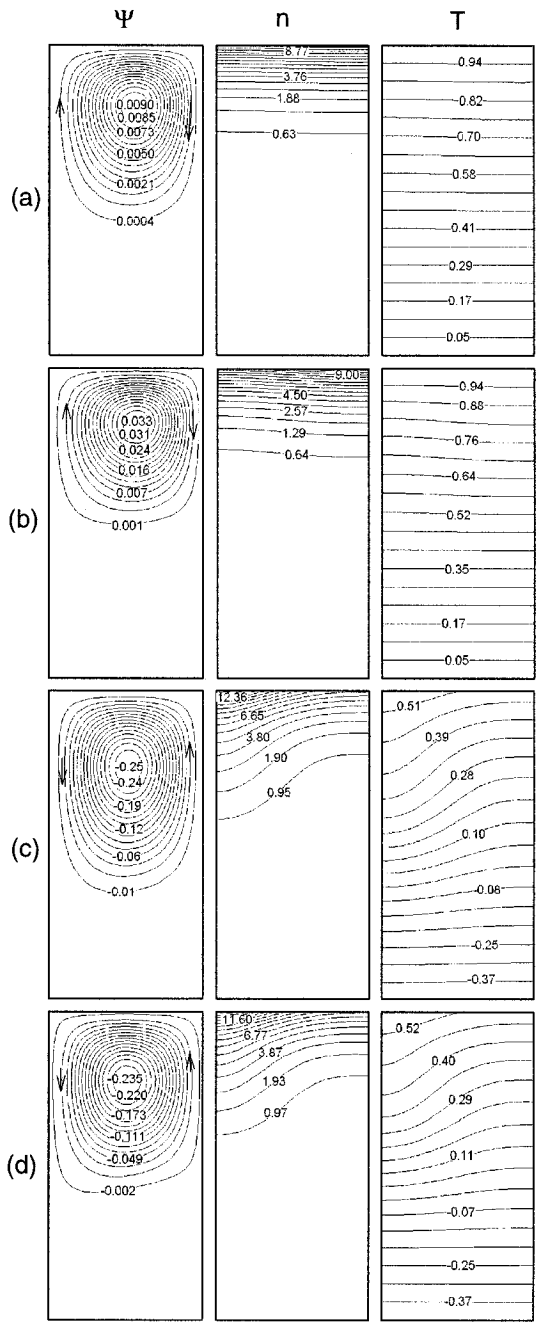

Figure 4.5 Streamlines, iso-concentration and isotherm near critical Rayleigh number for A=0.5, Pe=1. (a) T=constant, Ra_T=-1x Ra_{Tc}, Ra=3000 (b) T=constant, Ra_T=-2x Ra_{Tc}, Ra=3700 (c) q=constant, Ra_T=-1x Ra_{Tc}, Ra=2700 (d) q=constant, Ra_T=-2x Ra_{Tc}, Ra=3270.

A single convection cell circulates clockwise when cooling from below at constant temperature, Ψ_{ext} is 0.009 at Ra = 3,000, i.e. almost a diffusive state, the micro-organisms are accumulated almost uniformly at the top and the isotherms show a conduction regime. For cooling from below at constant heat flux, a single convection cell circulates counterclockwise, Ψ_{ext} is -0.25 at Ra = 2,700, the micro-organisms are accumulated at the top near $r = 0$ and the isotherms show a conduction regime with negative values at the bottom, positive values at the top. The case with Ra_T =-2xRa_{Tc} for both cooling from below at constant temperature and at constant heat flux is quite similar to the case with Ra_T =-1xRa_{Tc}: At Ra =3,700 and 3,270 for T or q constant respectively, corresponding Ψ_{ext} was 0.033 and -0.235, and iso-lines for concentration and temperature are almost identical to those with Ra_T =-1xRa_{Tc}. In contrast, we find identical iso-lines in the other cases with identical critical Rayleigh numbers for cooling from below at constant temperature or heat flux. Thus, we conclude that the reason for different critical Rayleigh numbers obtained in Figure 4.4 (b) could be an aspect ratio effect.

The onset of bioconvection with Ra_T = 0 is subcritical in all cases as shown in Figure 4.2 and transposed also in Figures 4.3 and 4.4. At Ra_T from -2xRa_{Tc} to +2xRa_{Tc}, the effect of the thermal Rayleigh number is to increase or decrease the convection, because the buoyancy forces developed are either cooperating or opposing the bioconvection. We see that for all cases considered in this study, the thermal effect Ra_T on the onset of the bioconvection is to make the subcritical bioconvection strongly supercritical.

A summary of the bifurcation diagrams for bioconvection and thermo-bioconvection including Ra_T and Ra_c values used at constant temperature and constant heat flux cases of Figures 4.3 and 4.4 are presented in Table 4.2. In this table, we listed the numerical values of the thermal Rayleigh number, Ra_T, the critical Rayleigh number of thermo-bioconvection, Ra_c, and the cases for which we could not obtain a diffusive state.

To examine the flow, concentration and temperature patterns at $Ra = 5\text{x}Ra_c$, streamlines and iso-concentration of selected cases at $Ra_T = 1\text{x } Ra_{Tc}$, $-1\text{x } Ra_{Tc}$ of Figures 4.3 and 4.4 are plotted in Figures 4.6-4.8, for $A = 1$, 0.5 and 0.2 respectively.

We present the case with $A = 1$, $Pe = 1$, $Ra = 5\text{x}Ra_c$ in Figure 4.6 (a-e). The case of bioconvection with $Ra_T = 0$ is shown as reference in (a), the circulation of convection cell is clockwise and $\Psi_{ext} = 2.20$. The convection cell is slightly asymmetric and transports the micro-organisms towards the upper corner near $r = A$. The cases with constant temperature heating and cooling are presented in Figure 4.6 (b,c). For $Ra_T = 1\text{x } Ra_{Tc}$, i.e. heating from below at constant temperature in Figure 4.6 (b), the thermal buoyancy forces are cooperating and the strength of convection is increased to $\Psi_{ext} = 2.67$. The concentration iso-lines are similar to those for bioconvection. The isotherms show high temperature gradients at the top center near $r = 0$. For $Ra_T = -1\text{x } Ra_{Tc}$, and for cooling from below at constant temperature in Figure 4.6 (c), the thermal buoyancy forces are opposing and the strength of convection is decreased to $\Psi_{ext} = 1.71$. The concentration

Table 4.2 Summary of bifurcation diagrams of Figures 4.3 and 4.4

CFB=cooling From Below, HFB=heating from below, No DS=No Diffusive State

Aspect Ratio	Pe	Temp/Flux	CFB /HFB	Ra_T	Ra_C	Remarks
A=1	Pe=1	q	CFB	$Ra_T=-2Ra_{Tc}=-3420$	5190	
				$Ra_T=-Ra_{Tc}=-1710$	3480	
			HFB	$Ra_T=Ra_{Tc}=1710$	≈ 0	
				$Ra_T=2Ra_{Tc}=3420$	--	No DS
		T	CFB	$Ra_T=-2Ra_{Tc}=-4540$	5160	
				$Ra_T=-Ra_{Tc}=-2270$	3480	
			HFB	$Ra_T=Ra_{Tc}=2270$	≈ 0	
				$Ra_T=2Ra_{Tc}=4540$	--	No DS
				$Ra_T=0$	1710	Bioconvection
	Pe=10	q	CFB	$Ra_T=-2Ra_{Tc}=-3420$	1350	
				$Ra_T=-Ra_{Tc}=-1710$	1100	
			HFB	$Ra_T=Ra_{Tc}=1710$	≈ 0	
				$Ra_T=2Ra_{Tc}=3420$	--	No DS
		T	CFB	$Ra_T=-2Ra_{Tc}=-4540$	1300	
				$Ra_T=-Ra_{Tc}=-2270$	1100	
			HFB	$Ra_T=Ra_{Tc}=2270$	≈ 0	
				$Ra_T=2Ra_{Tc}=4540$	--	No DS
				$Ra_T=0$	520	Bioconvection
A=0.5	Pe=1	q	CFB	$Ra_T=-2Ra_{Tc}=-20700$	29800	
				$Ra_T=-Ra_{Tc}=-10350$	20300	
			HFB	$Ra_T=Ra_{Tc}=10350$	≈ 0	
				$Ra_T=2Ra_{Tc}=20700$	--	No DS
		T	CFB	$Ra_T=-2Ra_{Tc}=-21600$	29400	
				$Ra_T=-Ra_{Tc}=-10800$	20000	
			HFB	$Ra_T=Ra_{Tc}=10800$	≈ 0	
				$Ra_T=2Ra_{Tc}=21600$	--	No DS
				$Ra_T=0$	10400	Bioconvection
	Pe=10	q	CFB	$Ra_T=-2Ra_{Tc}=-20700$	3250	
				$Ra_T=-Ra_{Tc}=-10350$	2600	
			HFB	$Ra_T=Ra_{Tc}=10350$	≈ 0	
				$Ra_T=2Ra_{Tc}=20700$	--	
		T	CFB	$Ra_T=-2Ra_{Tc}=-21600$	3500	
				$Ra_T=-Ra_{Tc}=-10800$	2910	
			HFB	$Ra_T=Ra_{Tc}=10800$	≈ 0	
				$Ra_T=2Ra_{Tc}=21600$	--	No DS
				$Ra_T=0$	2160	Bioconvection
A=0.2	Pe=1	q	CFB	$Ra_T=-2Ra_{Tc}=-596000$	749000	
				$Ra_T=-Ra_{T_c}=-298000$	514000	
			HFB	$Ra_T=Ra_{Tc}=298000$	≈ 0	
				$Ra_T=2Ra_{Tc}=-596000$	--	No DS
		T	CFB	$Ra_T=-2Ra_{Tc}=-598800$	731000	
				$Ra_T=-Ra_{Tc}=-299400$	509000	
			HFB	$Ra_T=Ra_{Tc}=299400$	≈ 0	
				$Ra_T=2Ra_{Tc}=598800$	--	
				$Ra_T=0$	270000	Bioconvection
	Pe=10	q	CFB	$Ra_T=-2Ra_{Tc}=-596000$	38500	
				$Ra_T=-Ra_{Tc}=-298000$	29100	
			HFB	$Ra_T=Ra_{Tc}=298000$	≈ 0	
				$Ra_T=2Ra_{Tc}=-596000$	--	No DS
		T	CFB	$Ra_T=-2Ra_{Tc}=-598800$	36100	
				$Ra_T=-Ra_{Tc}=-299400$	29000	
			HFB	$Ra_T=Ra_{Tc}=299400$	≈ 0	
				$Ra_T=2Ra_{Tc}=598800$	--	No DS
				$Ra_T=0$	19000	Bioconvection

iso-lines are similar to those in case of (b). As expected, the isotherms show that temperature gradients at the top center near $r = 0$ slightly reduced. We present the cases for heating and cooling at constant heat flux in Figure 4.6 (d,e). For $Ra_T = 1\text{x } Ra_{Tc}$, i.e. heating from below at constant heat flux in Figure 4.6 (d), the thermal buoyancy forces are cooperating and the strength of convection is increased to $\Psi_{ext} = 2.42$, which is slightly reduced with respect to that for heating from below at constant temperature in (b), though the concentration iso-lines are very similar to those in case (b). As expected, the isotherms are completely different with lower temperature gradients changing sign at approximately mid-plane. At $Ra_T = -1\text{x } Ra_{Tc}$, and for cooling from below at constant heat flux in Figure 4.6(e), the thermal buoyancy forces are opposing and the strength of convection is decreased to $\Psi_{ext} = 1.96$, lower than that for bioconvection in (a) but higher than that in (c). The concentration iso-lines and the isotherms are similar to those in case of (d).

We present Ψ_{ext}, n, T for $A = 0.5$, $Pe = 1$, $Ra = 5\text{x}Ra_c$ in Figure 4.7 (a-d). The cases (a) and (b) are for heating and cooling below at constant temperature and (c) and (d) for heating and cooling from below at constant heat flux. We note that for bioconvection in this case (not shown here), we had a single clockwise circulating convection cell with $\Psi_{ext} = -0.92$ and the micro-organisms accumulated at the top center near $r = 0$. We see in Figure 4.7 (a) that for $Ra_T = 1\text{x}Ra_{Tc}$, the single convection cell is circulating counterclockwise, almost symmetric. Its strength is $\Psi_{ext} = -1.15$. Due to its circulation direction, going upward at the center near $r = 0$, the micro-organisms are concentrated at

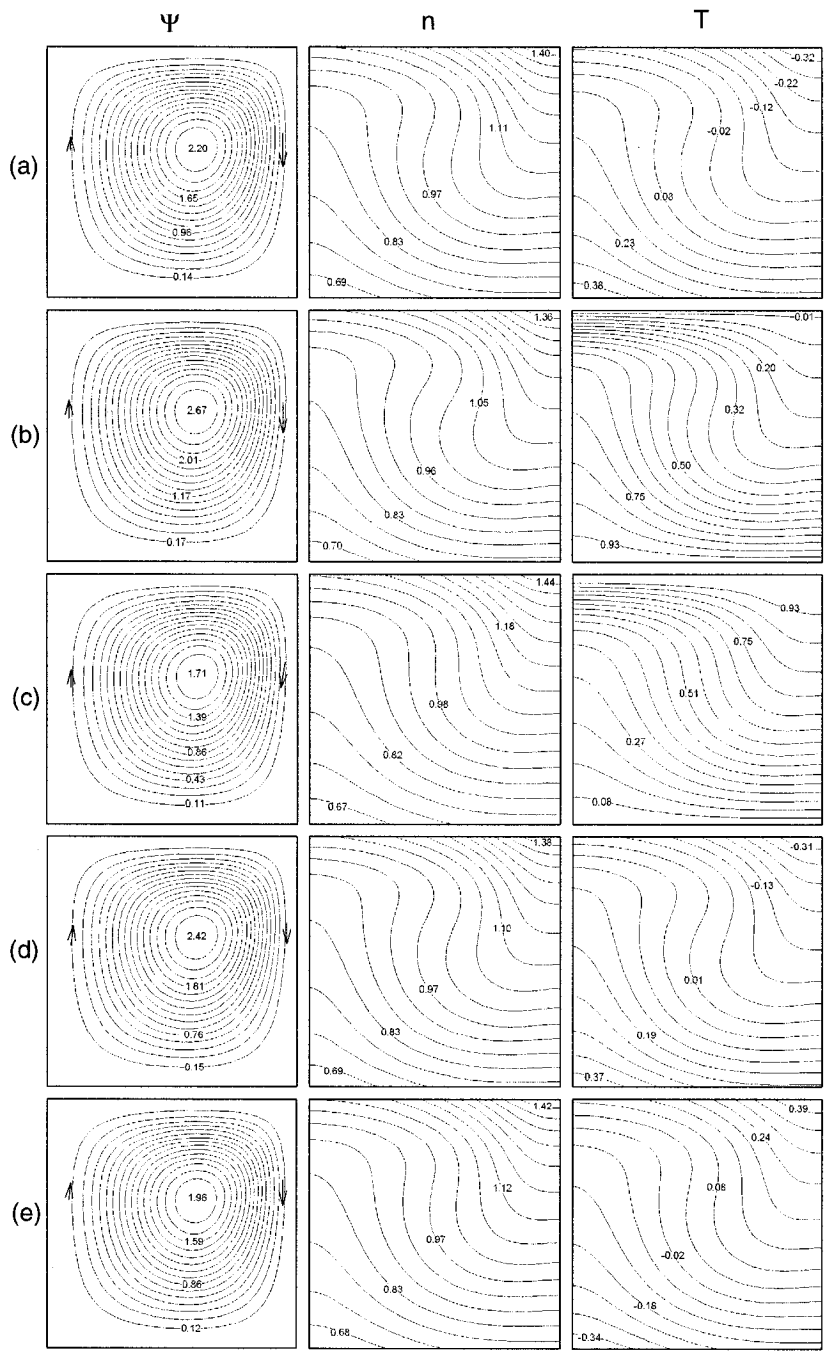

Figure 4.6 Streamlines, iso-concentration and isotherm for A=1, Pe=1 and Ra=5xRa_c. (a) Ra_T=0 (b) T=constant, Ra_T=1x Ra_{Tc} (c) T=constant, Ra_T=-1x Ra_{Tc} (d) q=constant, Ra_T=1x Ra_{Tc}, (e) q=constant, Ra_T=-1x Ra_{Tc}.

the center. As expected, the isotherms show high temperature gradients at the bottom and on the top right side. For Ra_T=-1xRa_{Tc} in Figure 4.7 (b), i.e. in cooling from below at constant temperature, in contrast to that of Figure 4.7 (a), the circulation of the single convection cell is clockwise and the circulation strength is reduced to Ψ_{ext} = 0.73, because of opposing thermal buoyancy forces. However, the iso-concentration is almost the same with micro-organisms at the right upper corner near $r = A$. The isotherms are almost a mirror image of those in (a) with high temperature gradients at the top center.

The results for heating and cooling from below at constant heat flux are presented in Figure 4.7 (c-d). We see for Ra_T = 1xRa_{Tc} in Figure 4.7 (c) that we have a counterclockwise circulating single convection cell with a circulation strength of Ψ_{ext} = -1.03. Consequently the micro-organisms are concentrated at the center near $r = 0$. Both streamlines and iso-concentration lines are similar to the case with constant temperature. The isotherms are with smaller temperature gradients, positive at the bottom and negative at the top, a typical characteristic for constant heat flux case. For Ra_T = -1xRa_{Tc} in Figure 4.7 (d), i.e. cooling from below at constant heat flux, the flow and concentration fields as well as the isotherms are similar to those in (c) but the circulation strength is reduced to Ψ_{ext}= -0.79, the concentration at the top is slightly increased and the isotherms are positive at the top and negative at the bottom. We note that in this case, we still have a counterclockwise circulation and for this reason the pattern did not change much with respect to the case (c).

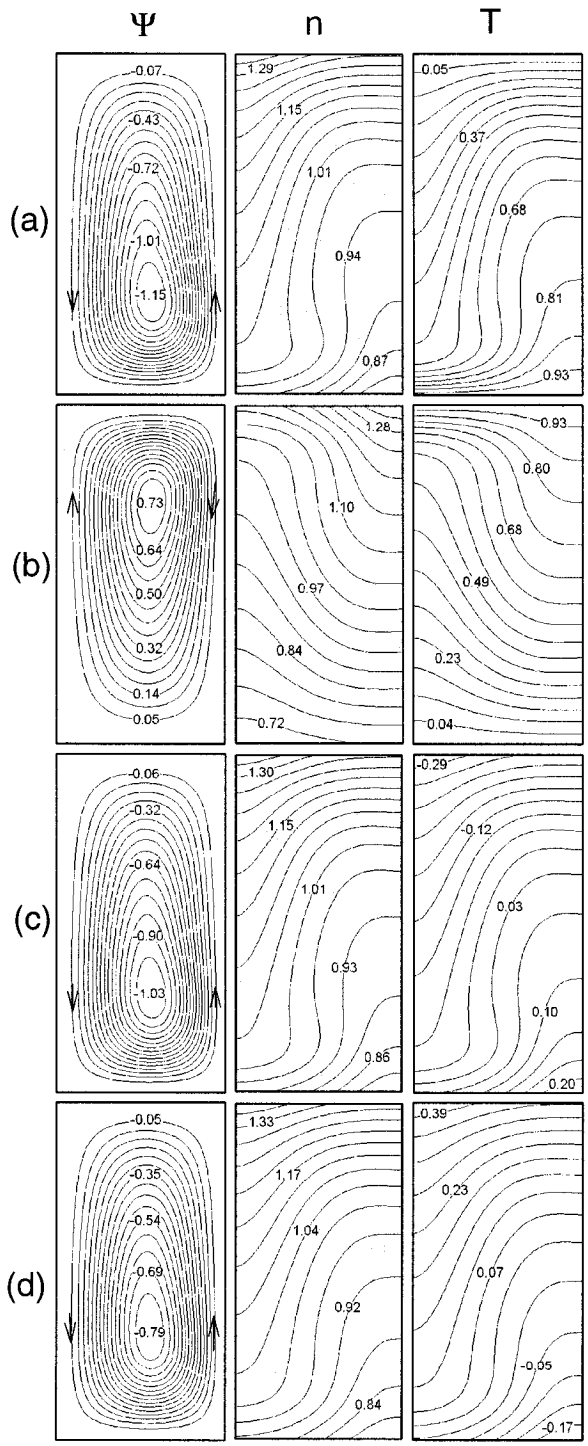

Figure 4.7 Streamlines, iso-concentration and isotherm for A=0.5, Pe=1 and Ra=5xRa_c. (a) T=constant, Ra_T=1x Ra_{Tc} (b) T=constant, Ra_T=-1x Ra_{Tc} (c) q=constant, Ra_T=1x Ra_{Tc}, (d) q=constant, Ra_T=-1x Ra_{Tc}.

We present Ψ_{ext}, n, T for $A = 0.2$, $Pe = 1$, $Ra = 5\text{x}Ra_c$ in Figure 4.8 (a-d). Heating and cooling from below at constant temperature are in Figure 4.8 (a,b) and those at constant heat flux in Figure 4.8 (c,d). We note that for bioconvection in this case (not shown here), we had two counter rotating convection cells, the lower one in counterclockwise circulation with $\Psi_{ext} = -0.16$ and the upper one in clockwise circulation with $\Psi_{ext} = 0.34$. The micro-organisms were accumulated at the top right corner with some stratification at the two counter rotating convection cells. For $Ra_T = 1\text{x}Ra_{Tc}$, i.e. heating from below in Figure 4.8 (a), we have two counter rotating cells, the lower one counterclockwise circulating with a strength of $\Psi_{ext} = -0.29$ and the clockwise circulating upper one with a strength of $\Psi_{ext} = 0.44$. Following circulation direction, the micro-organisms are concentrated mainly on the top right corner near $r = A$, and the isotherms show high temperature gradients at the bottom and top center. The appearance of flow and concentration fields is exactly similar to those for bioconvection with increased strength. For $Ra_T = -1\text{x}Ra_{Tc}$, i.e. cooling from below, in Figure 4.8 (b), a single clockwise circulating convection cell fills the cavity with the circulation strength of $\Psi_{ext} = 0.25$. The iso-concentration as well as the isotherms is quasi-stratified. Following circulation direction, the micro-organisms concentration is highest at the top right corner.

The case with heating and cooling at constant heat flux is presented in Figure 4.8 (c,d). For $Ra_T = 1\text{x}Ra_{Tc}$, i.e. heating from below, in Figure 4.8 (c), similar to that in (a), we have two counter rotating convection cells, the lower one counterclockwise circulating

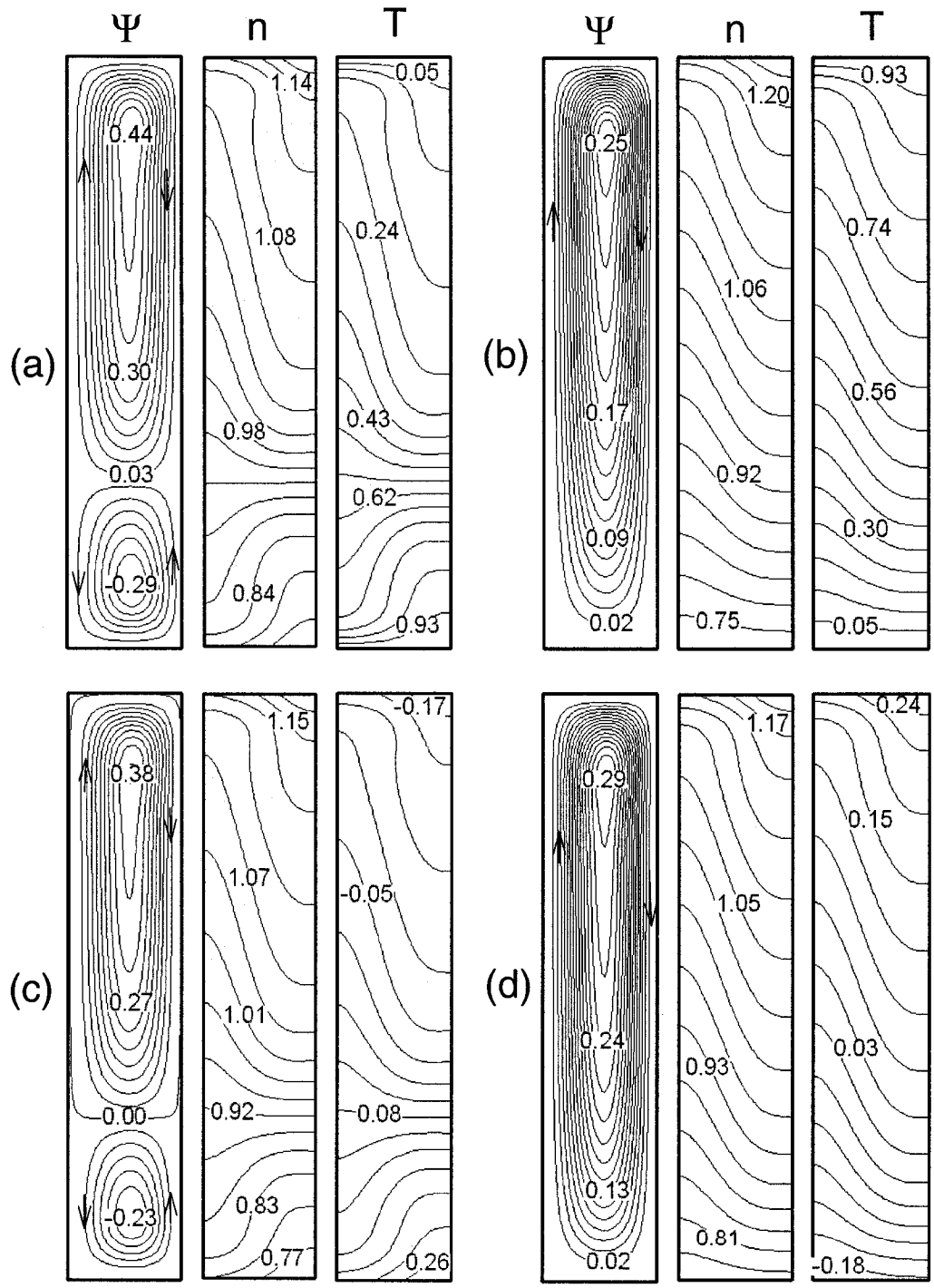

Figure 4.8 Streamlines, iso-concentration and isotherm for A=0.2, Pe=1 and Ra=5xRa_c. (a) T=constant, Ra_T=1xRa_{Tc} (b) T=constant, Ra_T=-1x Ra_{Tc} (c) q=constant, Ra_T=1x Ra_{Tc}, (d) q=constant, Ra_T=-1x Ra_{Tc}.

with a strength of Ψ_{ext}=-0.23 and the upper one clockwise circulating with a strength of Ψ_{ext} = 0.38. Patterns of iso-concentration lines and isotherms are very similar to those in Figure 4.8 (a), except the isotherms are positive on the bottom corresponding to the counterclockwise rotating convection cell and negative on the top corresponding to the clockwise rotating convection cell. For Ra_T = -1xRa_{Tc}, i.e. cooling from below, in Figure 4.8 (d), the patterns are similar to those in (b) with a single clockwise circulating convection cell filling the cavity with the circulation strength reduced to Ψ_{ext} = 0.29. The iso-concentration and the isotherms are quasi-stratified. Following circulation direction, the micro-organisms concentration is highest at the top right corner. Similar to the case in (c), the isotherms are in this case negative at the bottom and positive in the upper part.

4.3 Conclusion

Numerical simulations of thermo-bioconvection in vertical cylinders are carried out. The vertical walls of the cavity are assumed to be stress-free and insulated, while horizontal boundaries are rigid. For heating and cooling from below at constant temperature, the horizontal boundaries were maintained at fixed temperatures. For heating and cooling from below at constant heat flux, a constant heat flux through the horizontal boundaries was maintained. The governing equations are integrated numerically using the control volume method.

The results show the influence of thermal effect on the bifurcation diagram and the pattern of gravitactic bioconvection. We found that subcritical bifurcations of bioconvection became supercritical when the thermal Rayleigh number Ra_T is different than zero. For $Ra_T < 0$, i.e. for cooling from below, we have opposing buoyancy forces, the convection is decreased, the concentration iso-lines are modified to reflect the change in the flow field, and the critical thermo-bioconvection Rayleigh number is increased with respect to that of bioconvection. For $Ra_T > 0$, i.e. for heating from below, we have cooperating buoyancy forces, the convection is increased, the concentration iso-lines are changed, and the critical thermo-bioconvection Rayleigh number is decreased with respect to that of bioconvection. We found that both heating and cooling below at constant temperature and constant heat flux destabilize the gravitactic bioconvection.

Chapter 5

General Conclusions

Numerical simulations of bioconvection of gravitactic micro-organisms are carried out. In the first part at Chapter 3, the bioconvection in the rectangular cavity is investigated. The vertical walls of the cavity assumed to be stress-free and insulated, while horizontal boundaries are rigid. In the second part at Chapter 4, the thermo-bioconvection in the vertical cylinder is studied. The horizontal walls are kept at constant temperature or constant heat flux for the cooling and heating from bellow at constant temperature or constant heat flux, respectively. The governing equations are integrated numerically using the control volume method.

The results presented in Chapter 3 show the influence of bioconvection Peclet number and aspect ratio on the bifurcation diagram and the flow structure. We have found that the bifurcation remains subcritical in all cases when the bioconvection Pe number is varied from 0.1 to 10 in rectangular enclosures having an aspect ratio from 1 to 5.

The results presented in Chapter 4 show the influence of thermal effect on the bifurcation diagram and the pattern of gravitactic bioconvection. We found that subcritical bifurcations of bioconvection became supercritical when the thermal Rayleigh number Ra_T is different than zero. For $Ra_T < 0$, i.e. for cooling from below, we have opposing

buoyancy forces, the convection is decreased, the concentration iso-lines are modified to reflect the change in the flow field, and the critical thermo-bioconvection Rayleigh number is increased with respect to that of bioconvection. For $Ra_T > 0$, i.e. for heating from below, we have cooperating buoyancy forces, the convection is increased, the concentration iso-lines are changed, and the critical thermo-bioconvection Rayleigh number is decreased with respect to that of bioconvection. We found that both heating and cooling below at constant temperature and constant heat flux destabilize the gravitactic bioconvection.

References

[1] A.M. Metcalfe, T.J. Pedley, Falling plumes in bacterial bioconvection, J. Fluid Mech. 445 (2001) 121-149.

[2] A.J. Hillesdon, T.J. Pedley, Bioconvection in suspensions of oxytactic bacteria: linear theory, J. Fluid Mech. 324 (1996) 223-259.

[3] N.A. Hill, T.J. Pedley, J.O. Kessler, The growth of bioconvection patterns in a suspension of gyrotactic micro-organisms in a layer of finite depth, J. Fluid Mech. 208 (1989) 509-543.

[4] T.J. Pedley, J.O. Kessler, Hydrodynamic phenomena in suspensions of swimming micro-organisms, Ann. Rev. Fluid Mech. 24 (1992) 313-358.

[5] N.A. Hill, T.J. Pedley, Bioconvection, Fluid Dynamics Research 37 (2005) 1-20.

[6] S. Childress, M. Levandowsky, E.A. Spiegel, Pattern formation in a suspension of swimming micro-organisms: equations and stability theory, J. Fluid Mech. 63 (1975) 591-613.

[7] S. Fujita, M. Watanabe, Transition from periodic to non-periodic oscillation observed in a mathematical model of bioconvection by motile micro-organisms, Physica D: Nonlinear Phenomena 20 (1986) 435-443.

[8] A. Harashima, M. Watanabe, L. Fujishiro, Evolution of bioconvection patterns in a culture of motile flagellates, Phys. Fluids 31 (1988) 764-775.

[9] S. Ghorai, N.A. Hill, Development and stability of gyrotactic plumes in bioconvection, J. Fluid Mech. 400 (1999) 1-31.

[10] T.J. Pedley, N.A. Hill, J.O. Kessler, The growth of bioconvection patterns in a uniform suspension of gyrotactic micro-organisms, J. Fluid Mech. 195 (1988) 223-237.

[11] S. Ghorai, N.A. Hill, Wavelengths of gyrotactic plumes in bioconvection, Bull. Math. Biology 62 (2000) 429-450.

[12] M.A. Bees, N.A. Hill, Non-linear bioconvection in a deep suspension of gyrotactic swimming micro-organisms, J. Math. Biology 38(1999) 135-168.

[13] S. Childress, E.A. Spiegel, Pattern formation in suspension of swimming micro-organisms: Nonlinear aspects, in A Celebration of Mathematical Modeling: The Joseph B. Keller Anniversary Volume, D. Givoli, M.J. Grote, G.C. Papanicoulao, eds., Kluwer, Dordrecht 2004, pp.33-52.

[14] Z. Alloui, T.H. Nguyen, E. Bilgen, Bioconvection of gravitactic micro-organisms in vertical cylinder, Int. Comm. Heat and Mass Transfer 32 (2005) 739-747.

[15] A.V. Kuznetsov, The onset of bioconvection in a suspension of gyrotactic micro-organisms in a fluid layer of finite depth heated from below, Int. Comm. Heat and Mass Transfer 32 (2005) 574-582.

[16] A.V. Kuznetsov, Thermo-bioconvection in a suspension of oxytactic bacteria, Int. Comm. Heat and Mass Transfer 32 (2005) 991-999.

[17] A.V. Kuznetsov, Investigation of the onset of thermo-bioconvection in a suspension of oxytactic micro-organisms in a shallow fluid layer heated from below, Theor. Comput. Fluid Dyn. 19 (2005) 287-299.

[18] D.A. Nield, A.V. Kuznetsov, The onset of bio-thermal convection in a suspension of gyrotactic micro-organisms in a fluid layer: Oscillatory convection, Int. J. of Thermal Sciences, In Press.

[19] Z. Alloui, T.H. Nguyen, E. Bilgen, Stability analysis of thermo-bioconvection in suspensions of gravitactic micro-organisms in a fluid layer, Int. Comm. Heat and Mass Transfer, (2006).

[20] Z. Alloui, T.H. Nguyen, E. Bilgen, Numerical investigation of thermo-bioconvection in a suspension of gravitactic micro-organisms, Int. J. Heat and Mass Transfer, 50 (2007) 1439-1441.

[21] S.V. Patankar, Numerical heat transfer and fluid flow, McGraw Hill, New York (1980).

[22] A. Pellew, R.V. Southwell, On maintaining convective motion in a fluid heated from below, Proc. Royal Soc. Series A, Math. Phys. Sci. 176 (1940) 312-343.

[23] Z. Alloui, T.H. Nguyen, E. Bilgen, Numerical investigation of thermo-bioconvection in a suspension of gravitactic micro-organisms, Int. J. Heat and Mass Transfer, 50 (2007) 1439-1441.

[24] M. Taheri, E. Bilgen, Bioconvection of gravitactic micro-organisms in rectangular enclosures. Submitted to Int. J. Heat and Mass Transfer. November 7, 2006.

[25] T. Kawakubo, Y. Tsuchiya, Diffusion coefficient of paramecium as a function of temperature, J. Protozool. 28(3) (1981) 342-344.

[26] Y. Mogami, A. Yamane, A. Gino, S.A. Baba, Bioconvective pattern formation of *Tetrahymena* under altered gravity, The Journal of Experimental Biology 207 (2004) 3349.

[27] A. Pellew, R.V. Southwell, On maintaining convective motion in a fluid heated from below, Proc. R. Soc. Series A, Math. Phys. Sci. 176(1940) 312-343.

[28] Z. Alloui, T.H. Nguyen, E. Bilgen, Bioconvection of gravitactic micro-organisms in vertical cylinder, Int. Comm. Heat and Mass Transfer 32 (2005) 739-747.